

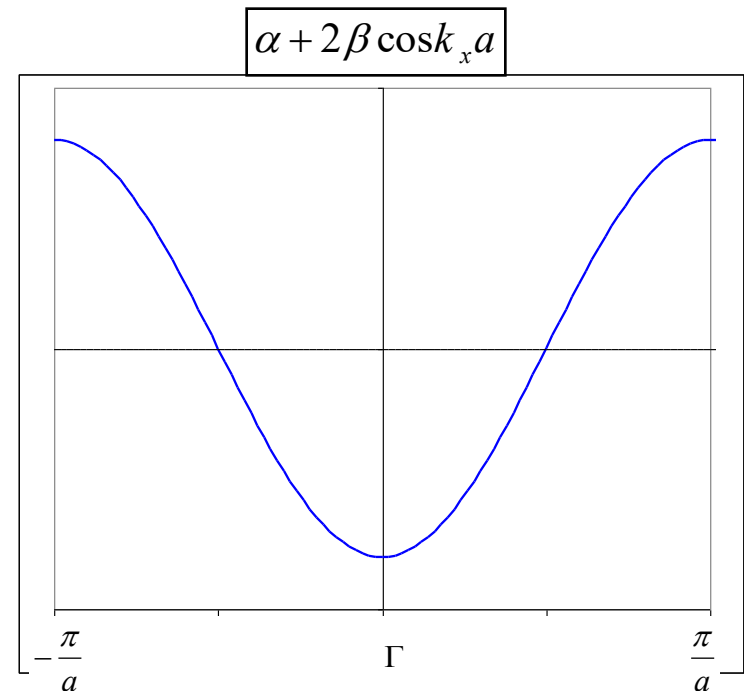
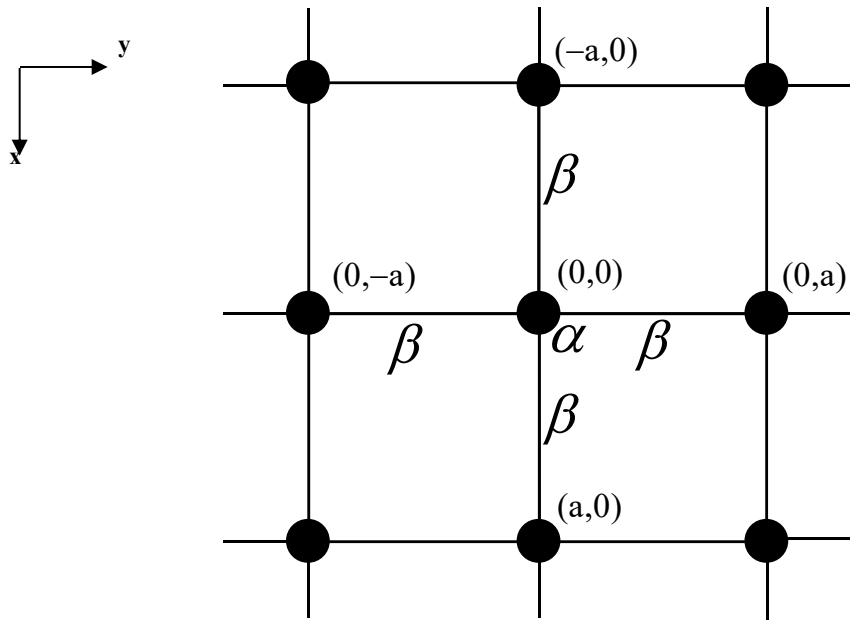
Uvažujeme jen interakce s nejbližšími sousedy:
jen překryvový integrál β s nejbližším sousedem

$$(E \sim \alpha, t \sim \beta, S \ll 1)$$

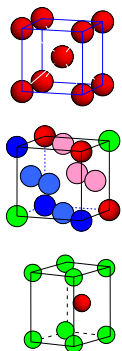
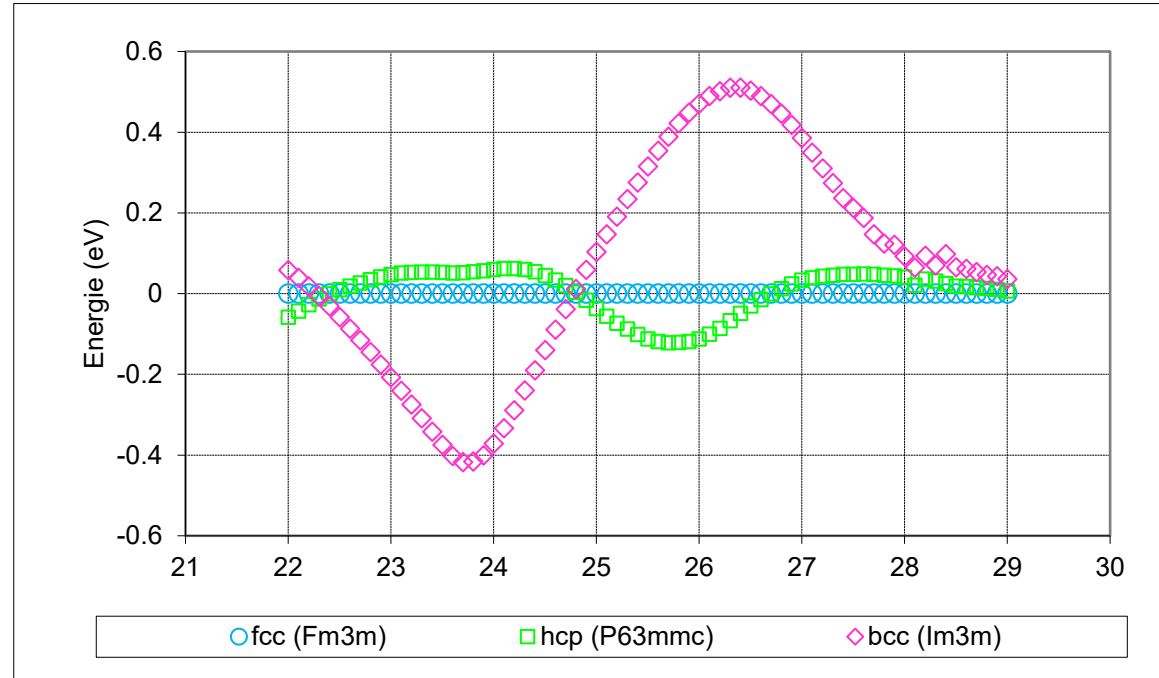
$$H(\vec{k}) = \alpha + \beta e^{ik_x a} + \beta e^{-ik_x a} = \alpha + 2\beta \cos k_x a$$

$$H(\vec{k}) = \alpha + \beta e^{ik_x a} + \beta e^{-ik_x a} + \beta e^{ik_y a} + \beta e^{-ik_y a} + \beta e^{ik_z a} + \beta e^{-ik_z a} =$$

$$= \alpha + 2\beta(\cos k_x a + \cos k_y a + \cos k_z a)$$



- Porovnání energií struktur fcc, hcp (jen ideální poměr a:c) a bcc
- Pro každou strukturu se spočítá závislost na objemu buňky a vybere se minimum.



bcc



ccp (fcc)



hcp

	21	22	23	24	25	26	27	28	29	30
3d	Sc	Ti	V	Cr	Mn	Fe	Co	Ni	Cu	Zn
4d	Y	Zr	Nb	Mo	Tc	Ru	Rh	Pd	Ag	Cd
5d	Lu	Hf	Ta	W	Re	Os	Ir	Pt	Au	Hg

1 IA New Original	2 IIA	3 IIIB	4 IVB	5 VB	6 VIB	7 VIIB	8	9 VIII	10	11 IB	12 IIB	13 IIIA	14 IVA	15 VA	16 VIA	17 VIIA	18 VIIIA
1 H Hydrogen 1.00794	2 He Helium 4.002602																
3 Li Lithium 6.941	4 Be Beryllium 9.012182											5 B Boron 10.811	6 C Carbon 12.0107	7 N Nitrogen 14.00674	8 O Oxygen 15.9994	9 F Fluorine 18.9984032	10 Ne Neon 20.1797
11 Na Sodium 22.989770	12 Mg Magnesium 24.3050											13 Al Aluminum 26.981538	14 Si Silicon 28.0855	15 P Phosphorus 30.973761	16 S Sulfur 32.066	17 Cl Chlorine 35.453	18 Ar Argon 39.948
19 K Potassium 39.0983	20 Ca Calcium 40.078	21 Sc Scandium 44.955910	22 Ti Titanium 47.867	23 V Vanadium 50.9415	24 Cr Chromium 51.9961	25 Mn Manganese 54.938049	26 Fe Iron 55.8457	27 Co Cobalt 58.933200	28 Ni Nickel 58.6934	29 Cu Copper 63.546	30 Zn Zinc 65.409	31 Ga Gallium 69.723	32 Ge Germanium 72.64	33 As Arsenic 74.92160	34 Se Selenium 78.96	35 Br Bromine 79.904	36 Kr Krypton 83.798
37 Rb Rubidium 85.4678	38 Sr Strontium 87.62	39 Y Yttrium 88.90585	40 Zr Zirconium 91.224	41 Nb Niobium 92.90638	42 Mo Molybdenum 95.94	43 Tc Technetium (98)	44 Ru Ruthenium 101.07	45 Rh Rhodium 102.90550	46 Pd Palladium 106.42	47 Ag Silver 107.8682	48 Cd Cadmium 112.411	49 In Indium 114.818	50 Sn Tin 118.710	51 Sb Antimony 121.760	52 Te Tellurium 127.60	53 I Iodine 126.90447	54 Xe Xenon 131.293
55 Cs Cesium 132.90545	56 Ba Barium 137.327	57 to 71	72 Hf Hafnium 178.49	73 Ta Tantalum 180.9479	74 W Tungsten 183.84	75 Re Rhenium 186.207	76 Os Osmium 190.23	77 Ir Iridium 192.217	78 Pt Platinum 195.078	79 Au Gold 196.96655	80 Hg Mercury 200.59	81 Tl Thallium 204.3833	82 Pb Lead 207.2	83 Bi Bismuth 208.98038	84 Po Polonium (209)	85 At Astatine (10)	86 Rn Radon (222)
87 Fr Francium (223)	88 Ra Radium (226)	89 to 103	104 Rf Rutherfordium (261)	105 Db Dubnium (262)	106 Sg Seaborgium (266)	107 Bh Bohrium (264)	108 Hs Hassium (269)	109 Mt Meitnerium (268)	110 Ds Darmstadtium (271)	111 Rg Roentgenium (272)	112 Uub Ununbium (285)	113 Uut Ununtrium (284)	114 Uuq Ununquadium (289)	115 Uup Ununpentium (288)	116 Uuh Ununhexium (292)	117 Uus Ununseptium	118 Uuo Ununoctium

- Alkali metals
- Alkaline earth metals
- Transition metals
- Lanthanide series
- Actinide series
- Poor metals
- Nonmetals
- Noble gases
- C Solid
- Br Liquid
- H Gas
- Tc Synthetic

Atomic masses in parentheses are those of the most stable or common isotope.

Design Copyright © 1997 Michael Dayah (michael@dayah.com) <http://www.dayah.com/periodic/>

Note: The subgroup numbers 1-18 were adopted in 1984 by the International Union of Pure and Applied Chemistry. The names of elements 112-118 are the Latin equivalents of those numbers.

57 La Lanthanum 138.9055	58 Ce Cerium 140.116	59 Pr Praseodymium 140.90765	60 Nd Neodymium 144.24	61 Pm Promethium (145)	62 Sm Samarium 150.36	63 Eu Europium 151.964	64 Gd Gadolinium 157.25	65 Tb Terbium 158.92534	66 Dy Dysprosium 162.500	67 Ho Holmium 164.93032	68 Er Erbium 167.259	69 Tm Thulium 168.93421	70 Yb Ytterbium 173.04	71 Lu Lutetium 174.967
89 Ac Actinium (227)	90 Th Thorium 232.0381	91 Pa Protactinium 231.03588	92 U Uranium 238.02891	93 Np Neptunium (237)	94 Pu Plutonium (244)	95 Am Americium (243)	96 Cm Curium (247)	97 Bk Berkelium (247)	98 Cf Californium (251)	99 Es Einsteinium (252)	100 Fm Fermium (257)	101 Md Mendelevium (258)	102 No Nobelium (259)	103 Lr Lawrencium (262)

	I	II
2	Li	Be
3	Na	Mg
4	K	Ca
5	Rb	Sr
6	Cs	Ba

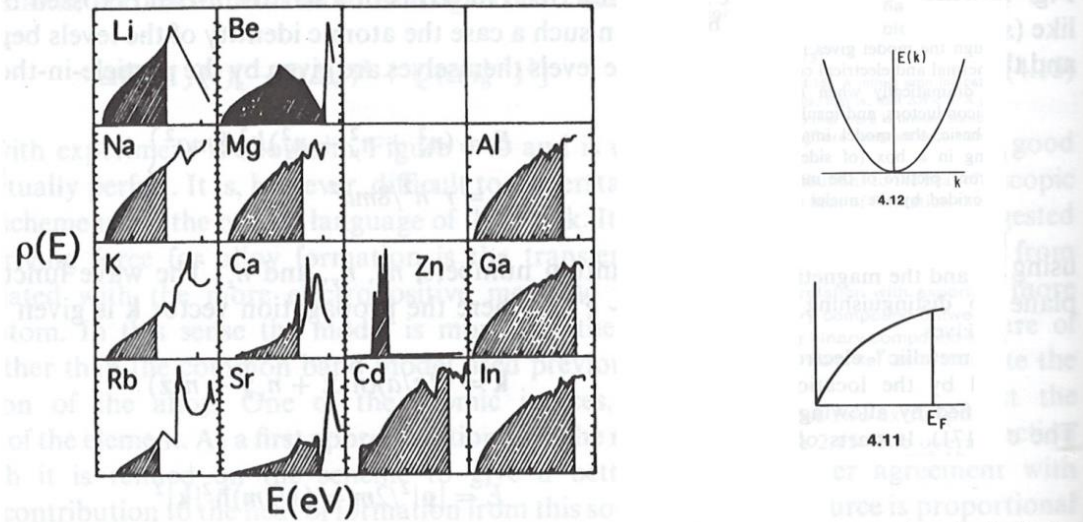
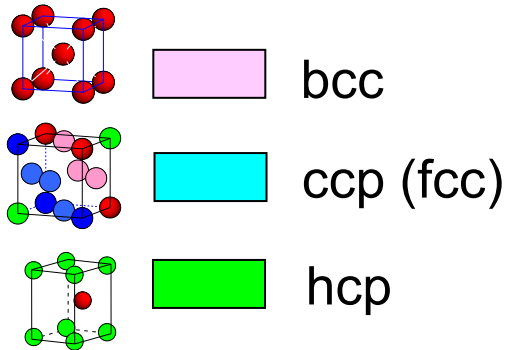


Figure 4.41 Densities of states for some of the sp (main group) metals, showing the similarity for many to that expected from the free-electron model. (Adapted from Ref. 288.)

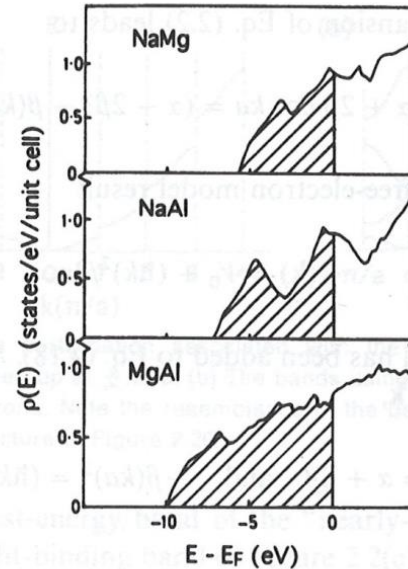
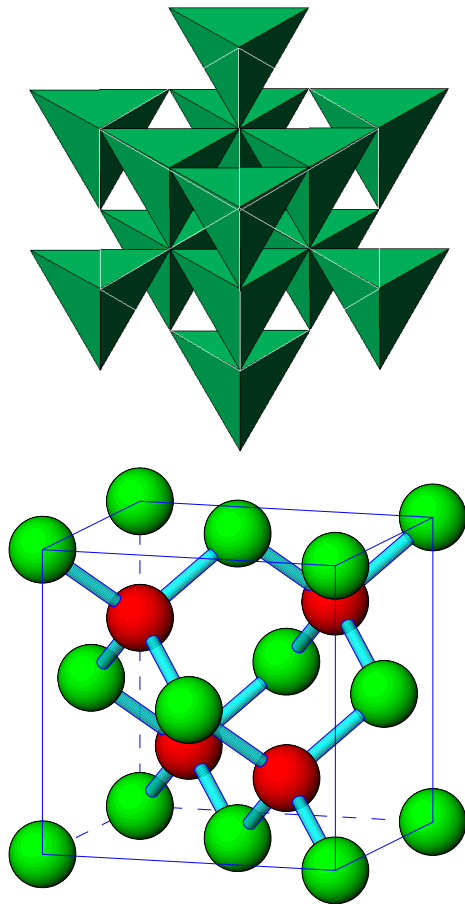
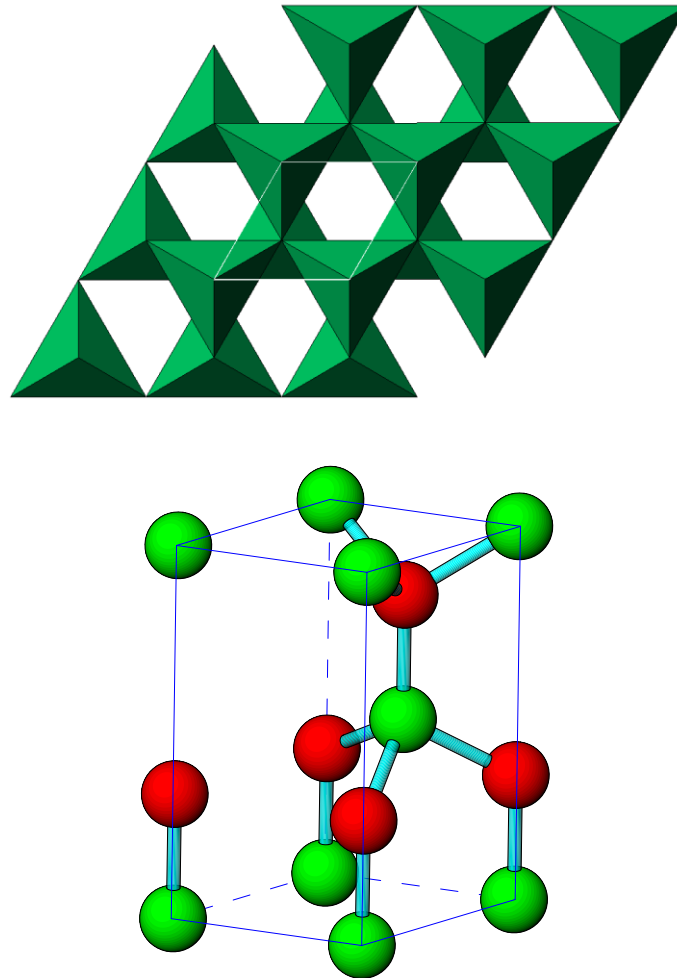


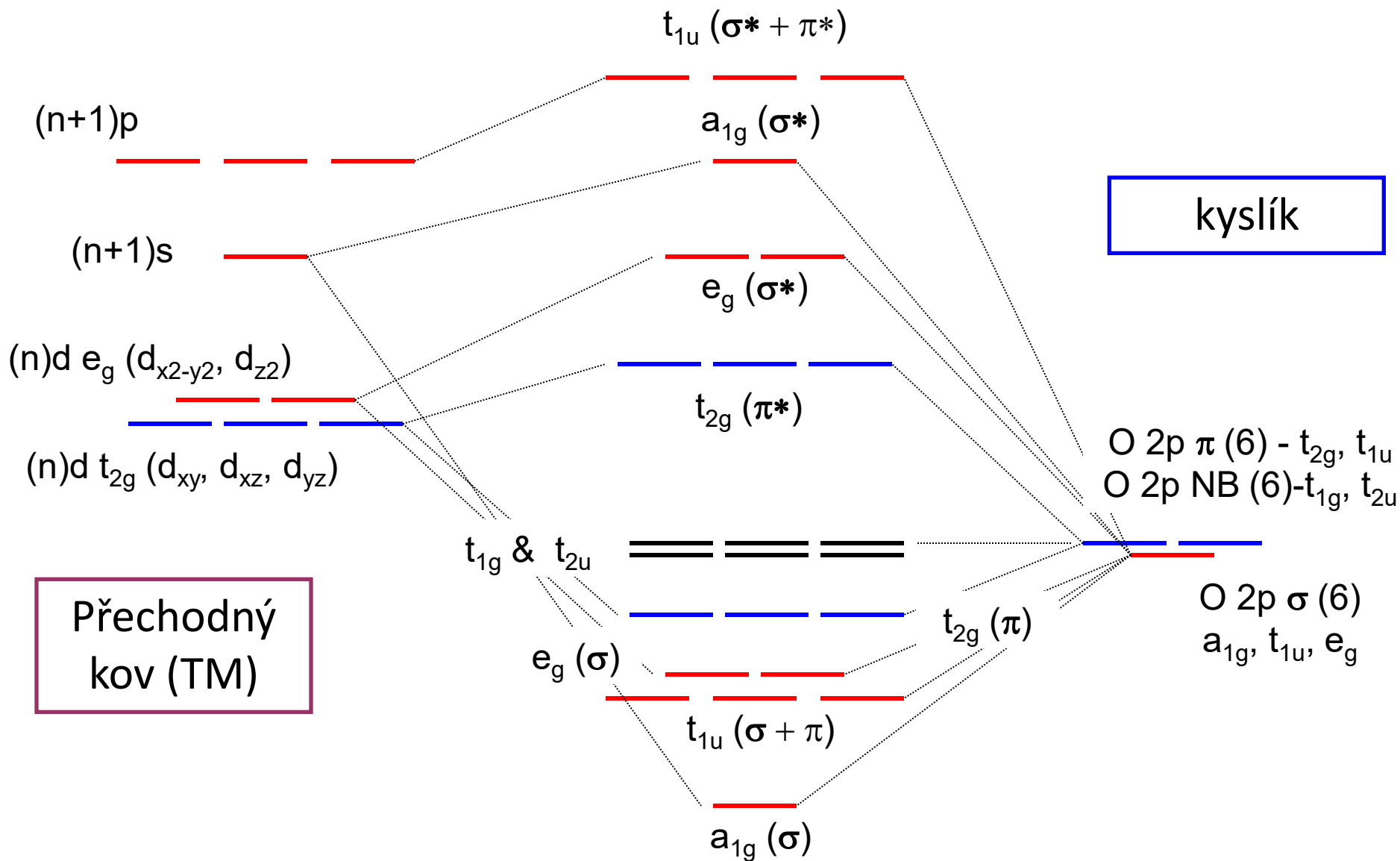
Figure 4.42 Densities of states for some alloys of the sp (main group) metals. The poorest agreement with the free-electron parabola is seen for NaAl, where there is the largest difference in Z and hence electronegativity. (Adapted from Ref. 288.)

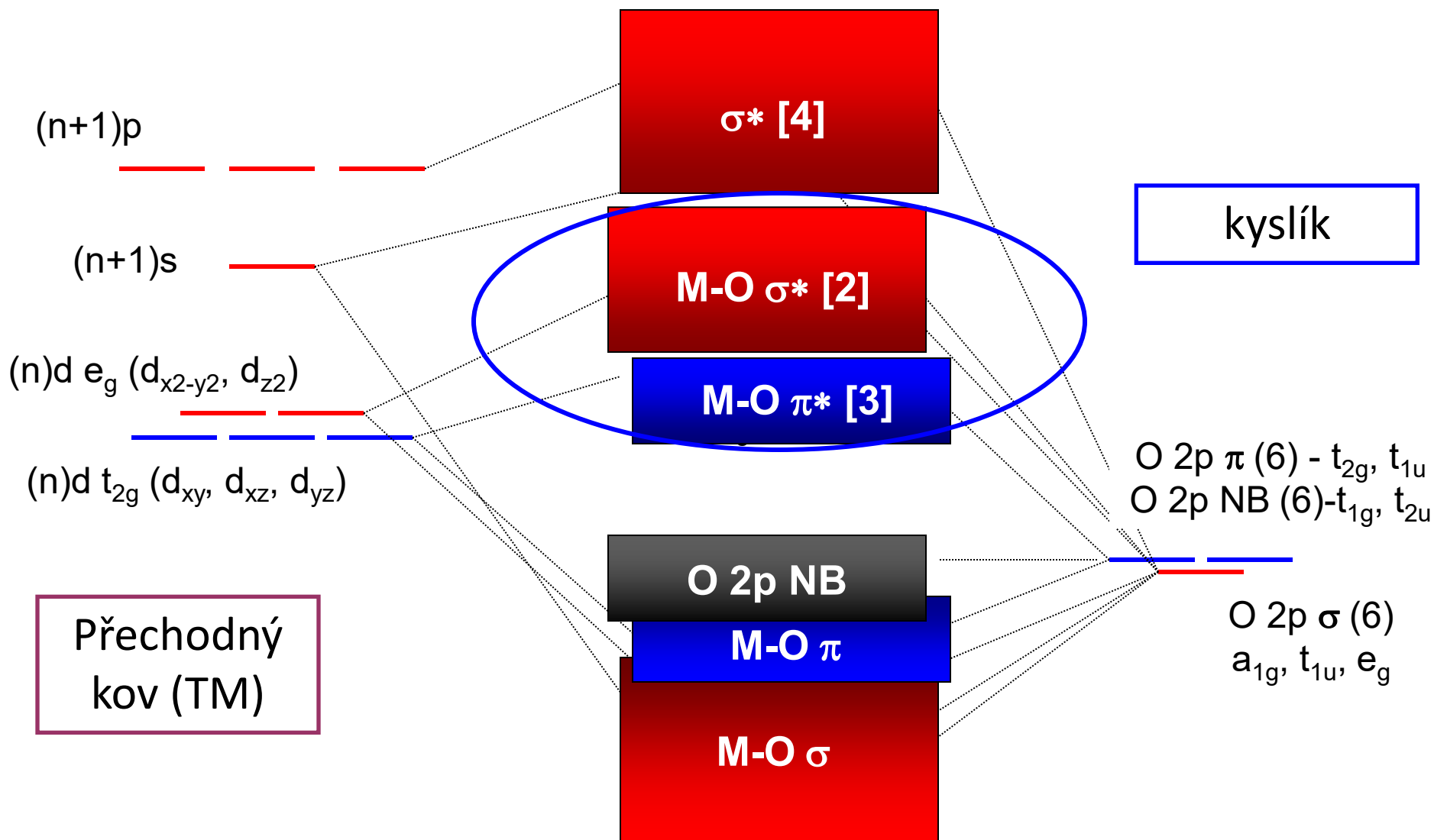
sfalerit ZnS, diamant, Si



wurtzit ZnS







X bod ($k_x = \pi/a, k_y = k_z = 0$)

$d_{xy}, d_{xz} \rightarrow$ antivazebné

$d_{yz} \rightarrow$ nevazebné

2 degenerované pásy

M bod ($k_x = k_y = \pi/a, k_z = 0$)

$d_{xy} \rightarrow$ antivazebné

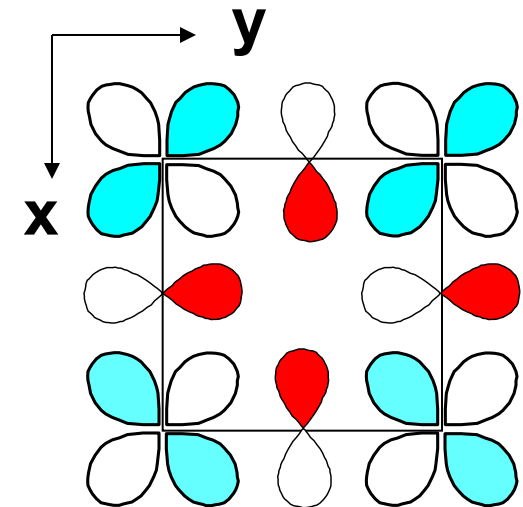
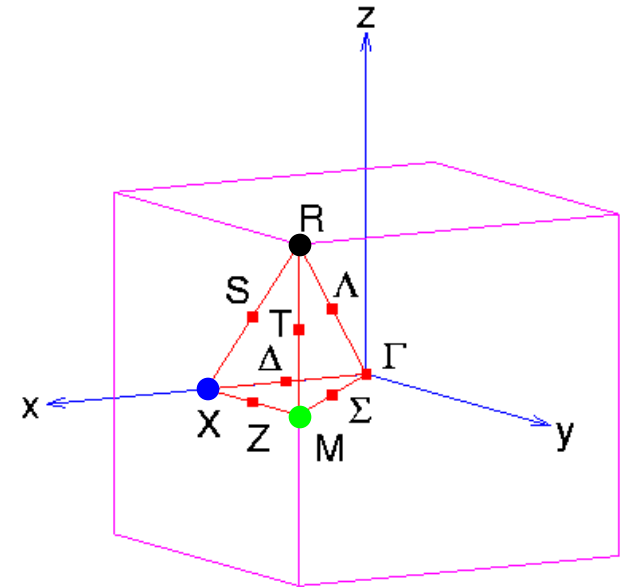
$d_{yz}, d_{xz} \rightarrow$ méně antivazebné

2 degenerované pásy

R bod ($k_x = k_y = k_z = \pi/a$)

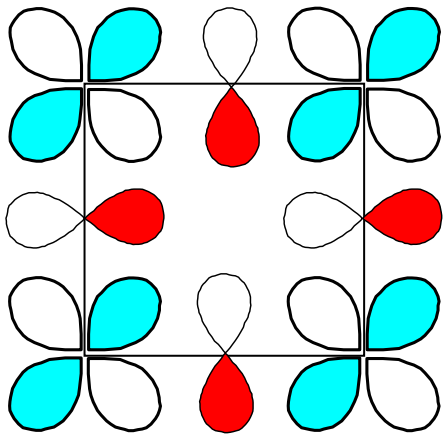
$d_{xy}, d_{yz}, d_{xz} \rightarrow$ antivazebné

3 degenerované pásy

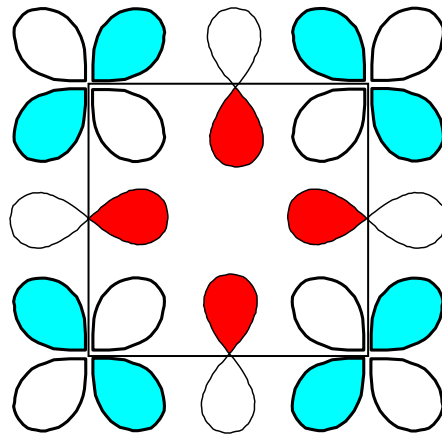


X bod

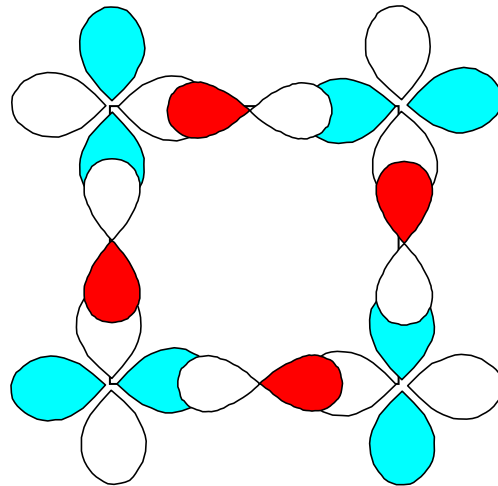
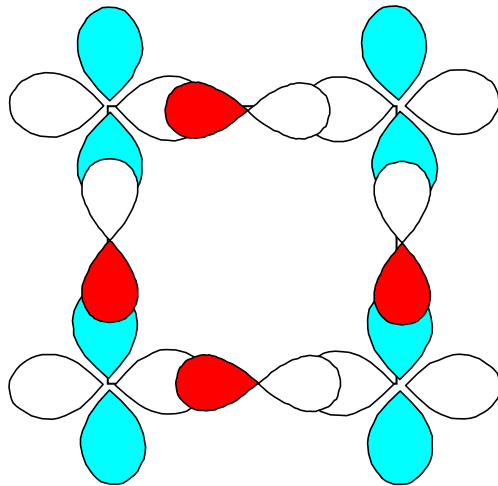
8



Γ bod
($k_x=k_y=0$)
nevazebné



M bod
($k_x=k_y=\pi/a$)
antivazebné



π^* - překryv (TM t_{2g} – O 2p π)

$\Gamma \rightarrow M$:

Energie pásu se zvyšuje

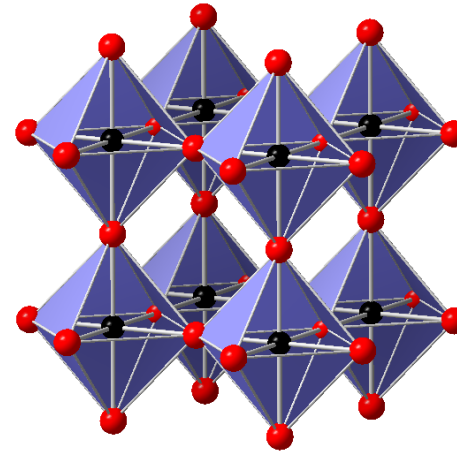
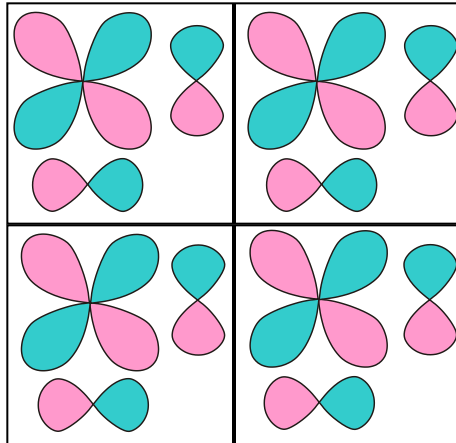
Větší překryv pro σ vazbu

$$W(\sigma^*) > W(\pi^*)$$

σ^* - překryv (TM e_g – O 2p σ)

$\Gamma \rightarrow M$:

Energie pásu se zvyšuje



ReO_3 :

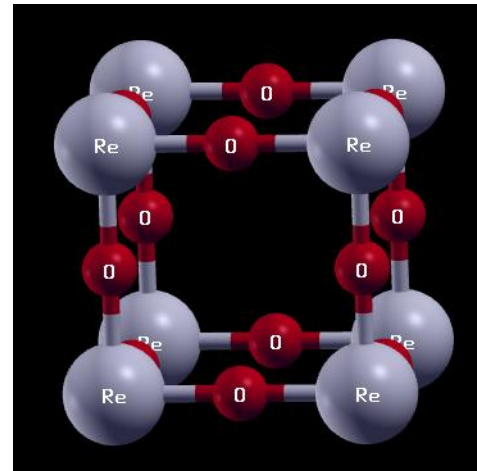
$\text{Re}^{6+} d^1$

π -vazby $t_{2g} - p$

$d_{xy} - p_x(y), p_y(x)$

$d_{xz} - p_x(z), p_z(x)$

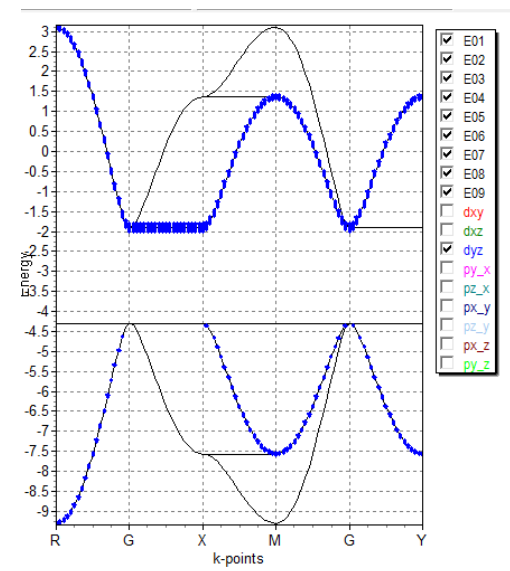
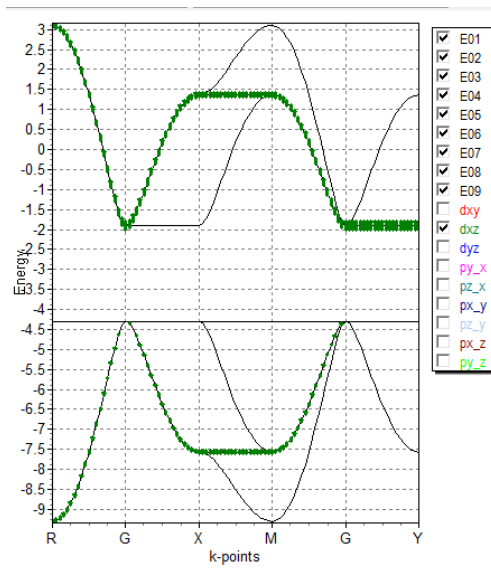
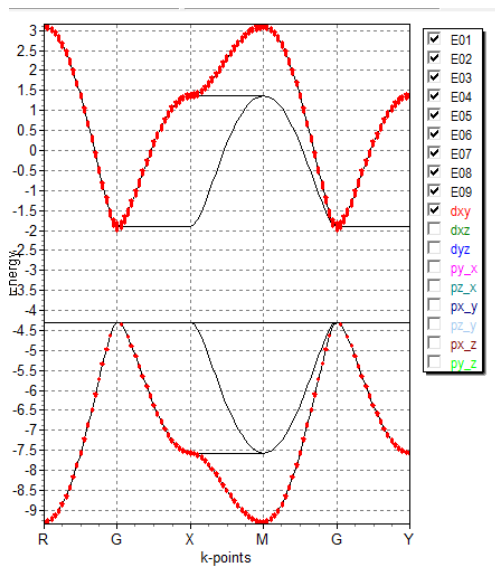
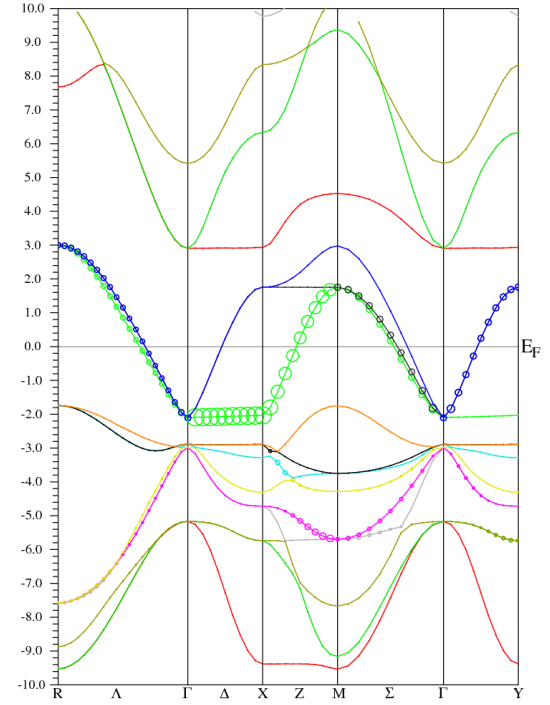
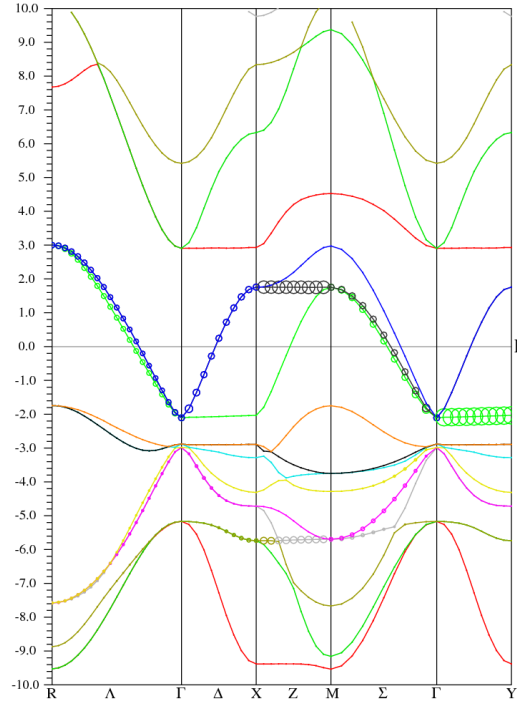
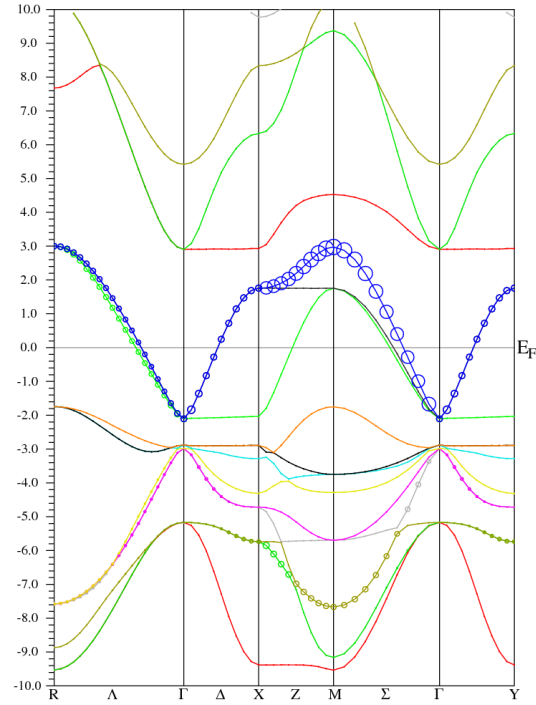
$d_{yz} - p_y(z), p_z(y)$



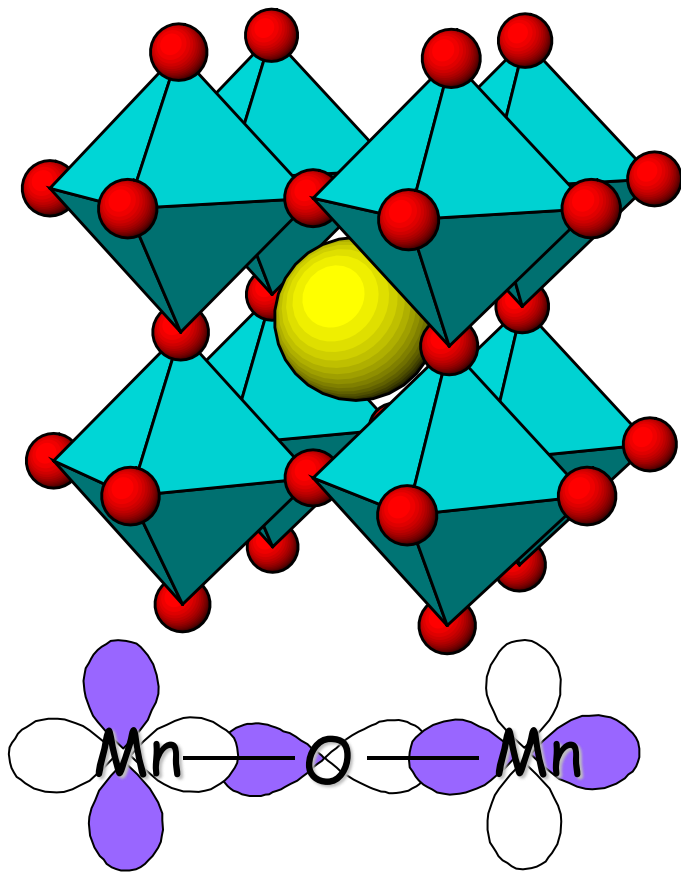
kipl atom 1DXY size 0.50

kipl atom 1DXZ size 0.50

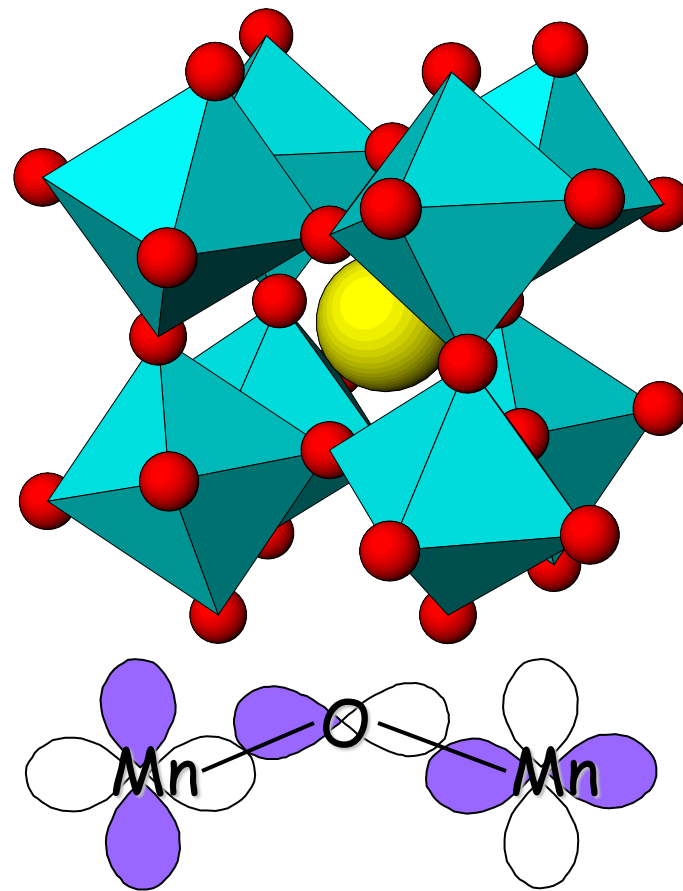
kipl atom 1DYZ size 0.50



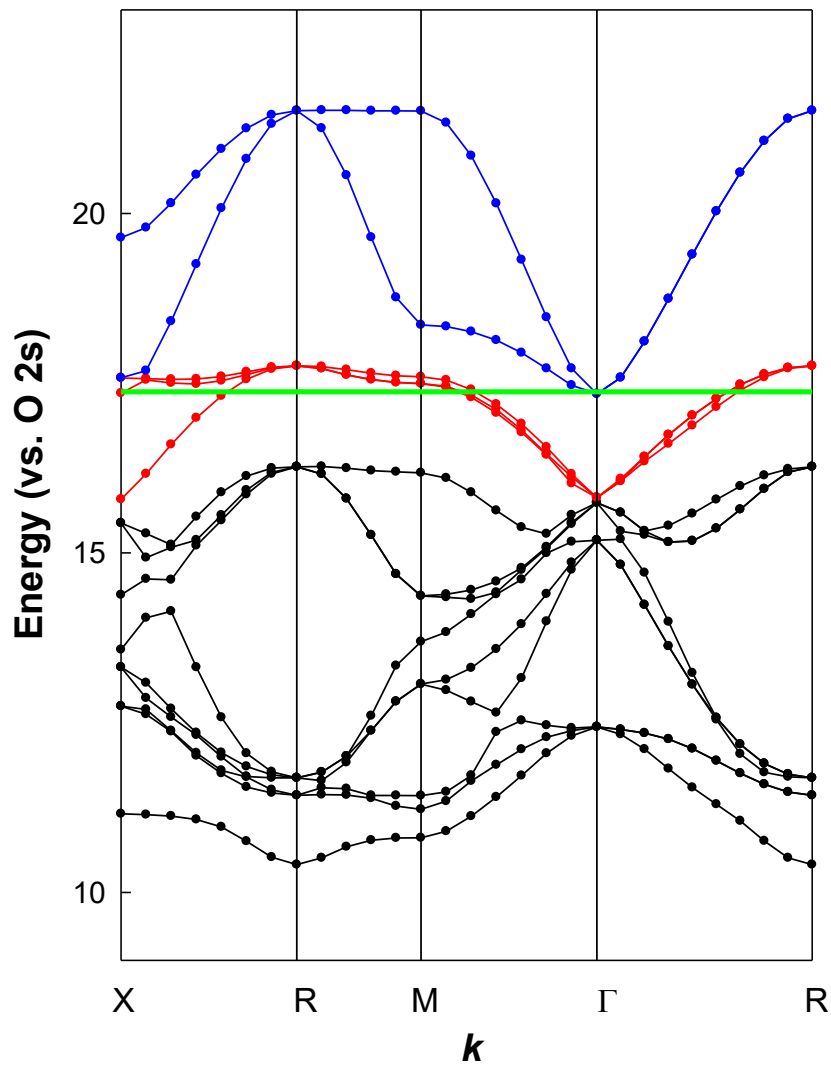
Kubický perovskit ($Pm\bar{3}m$)
úhel vazby Mn-O-Mn = 180°



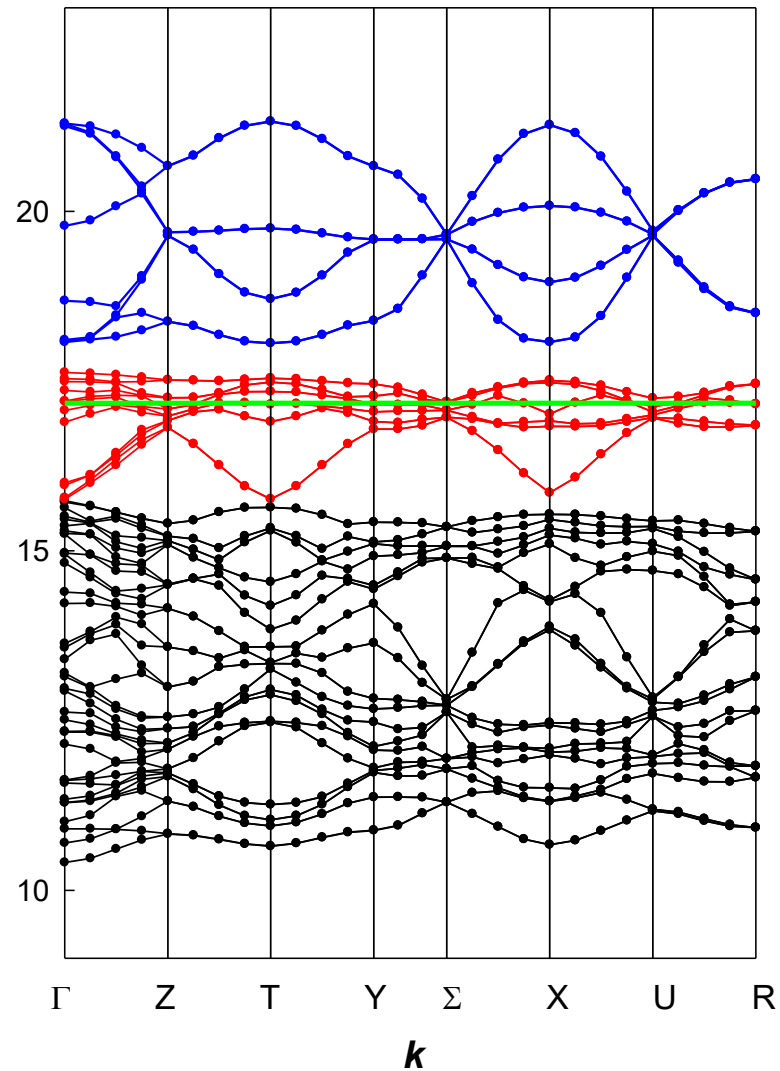
Orthorombický perovskit ($Pnma$)
úhel vazby Mn-O-Mn $< 180^\circ$

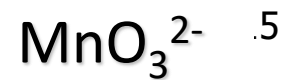
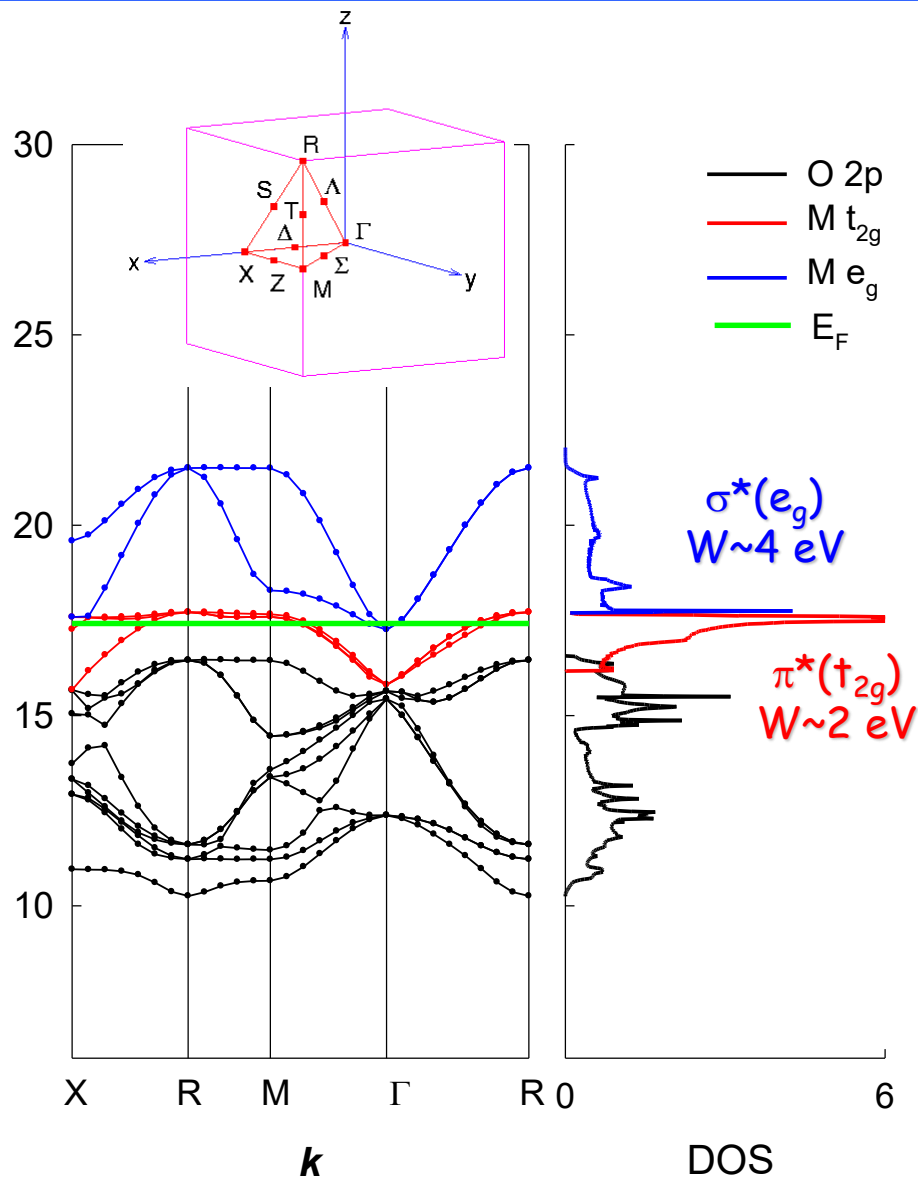
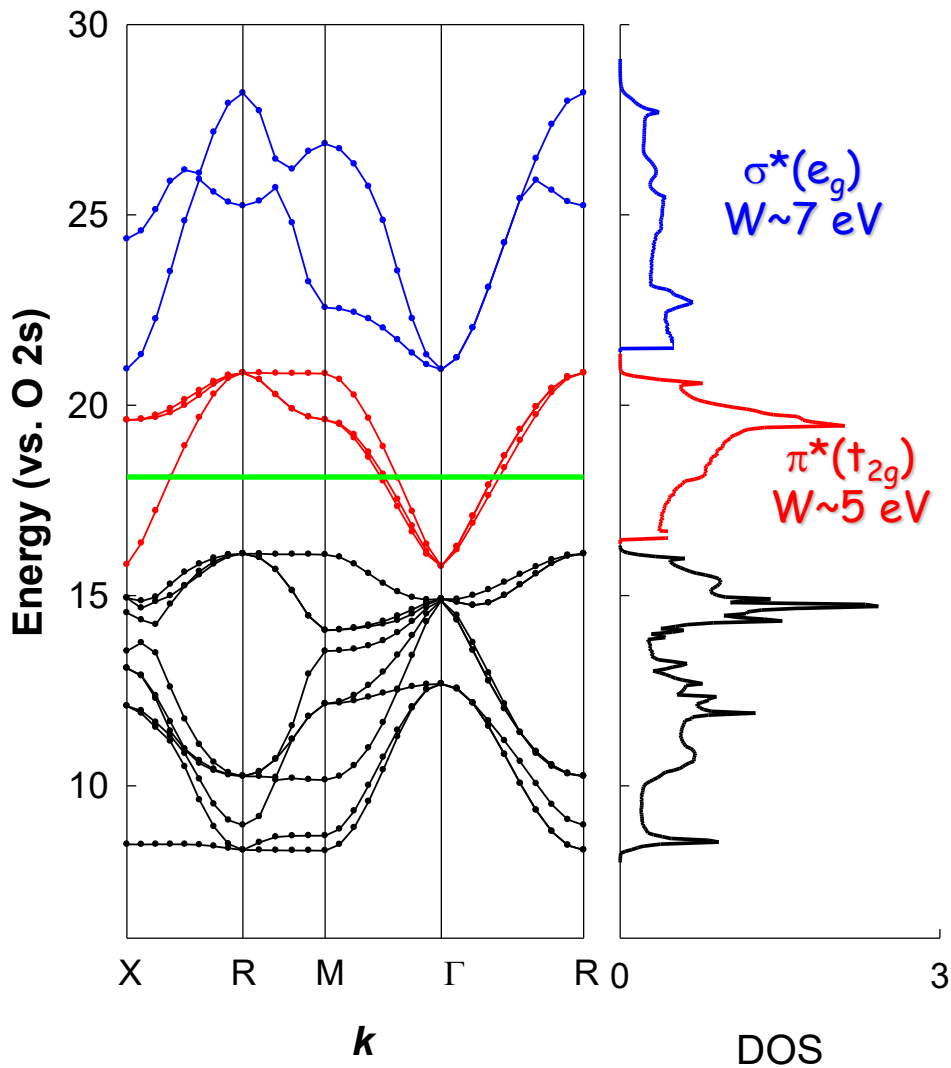


Kubický perovskit (Pm3m)
úhel vazby Mn-O-Mn = 180°



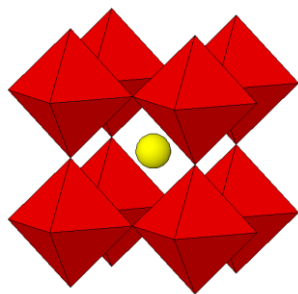
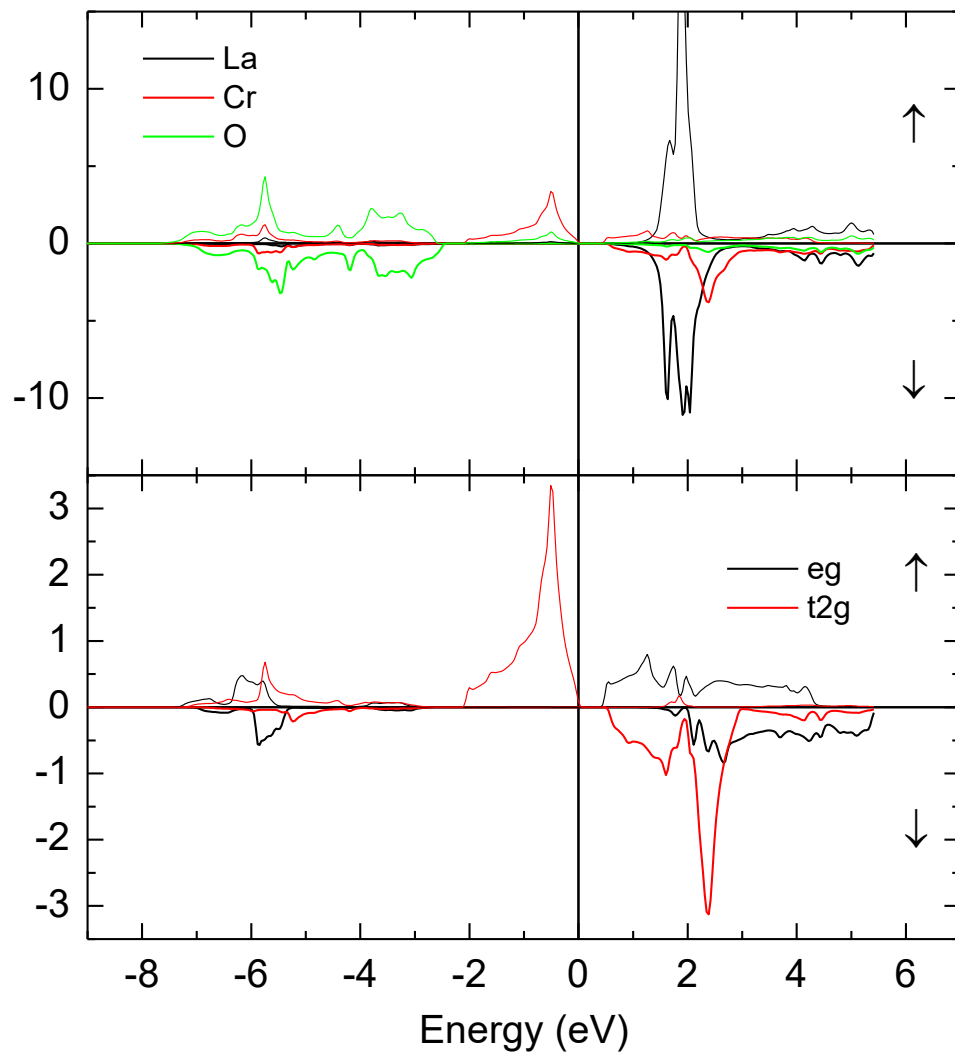
Orthorombický perovskit (Pnma)
úhel vazby Mn-O-Mn < 180°

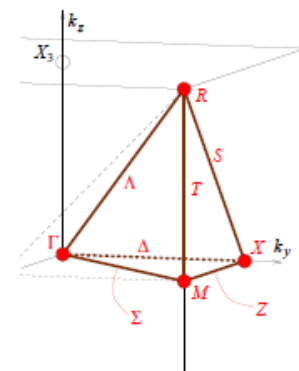
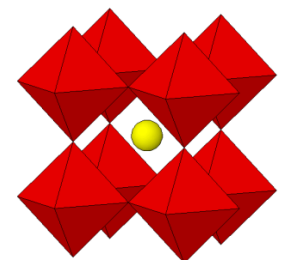
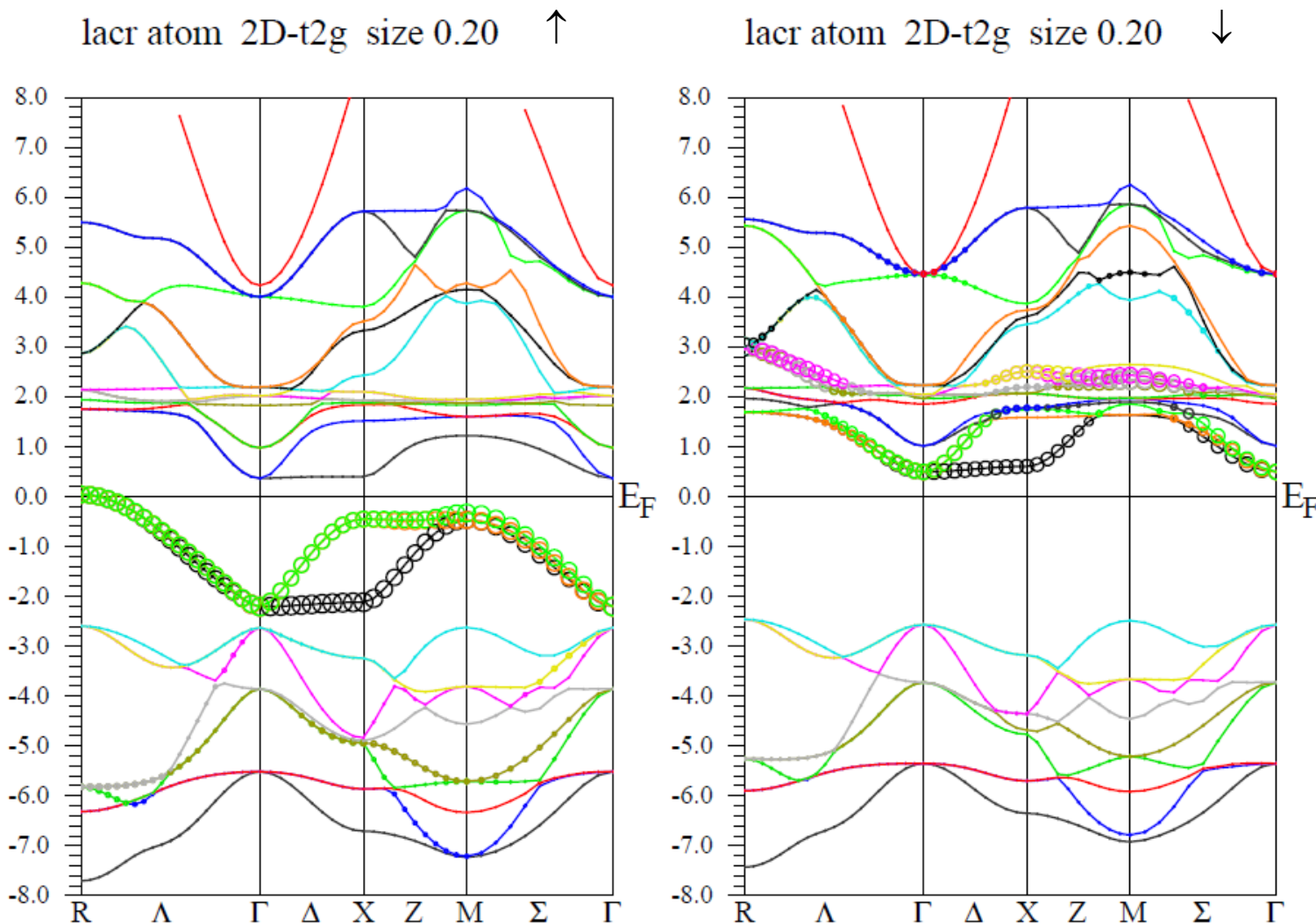




- Diagram molekulových orbitalů pro oktaedr
- $\pi^*(t_{2g})$ a $\sigma^*(e_g)$ pásy
- Překryv orbitalů a šířka pásu (ReO_3 vs. MnO_3^{2-})
- Strukturální deformace (náklon oktaedrů)
- Výměnná energie (Energie spárování spinů)
- Počet d-elektronů

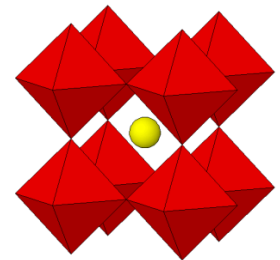
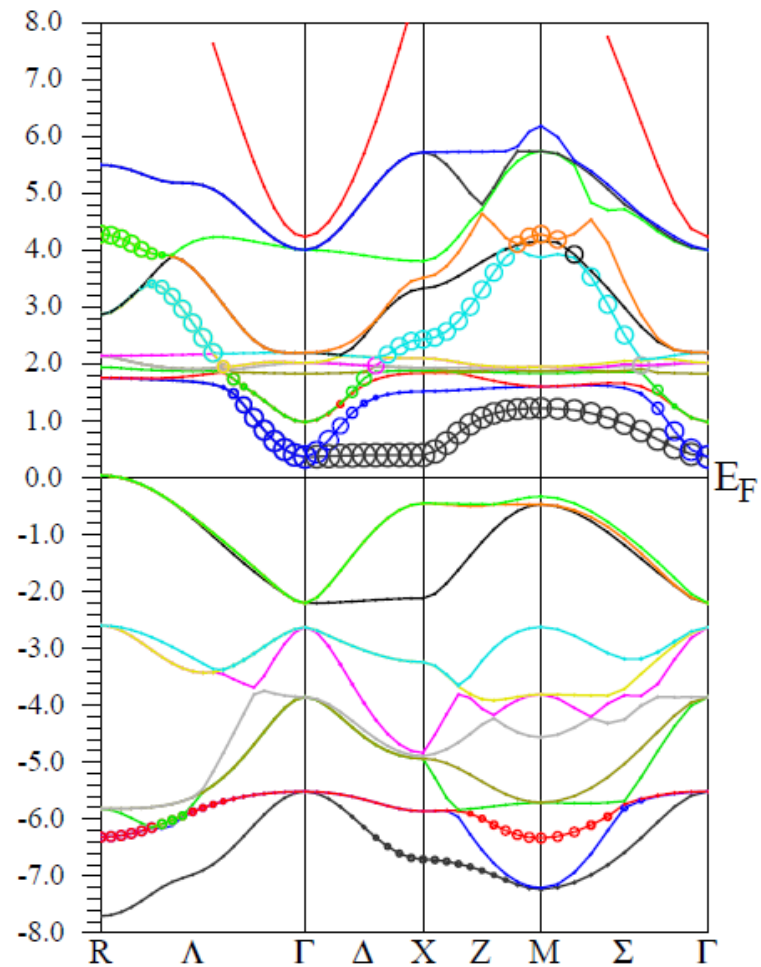
LaCrO₃
d³ – t_{2g}³



Figure 1: LaCrO₃, d³ – t_{2g}³, Cr-t_{2g}

lacr atom 2D-eg size 0.20 ↑

↓



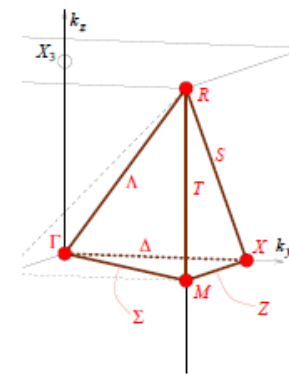
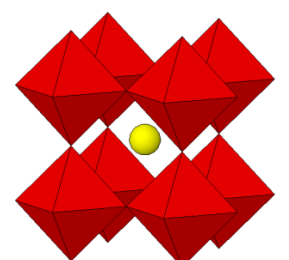
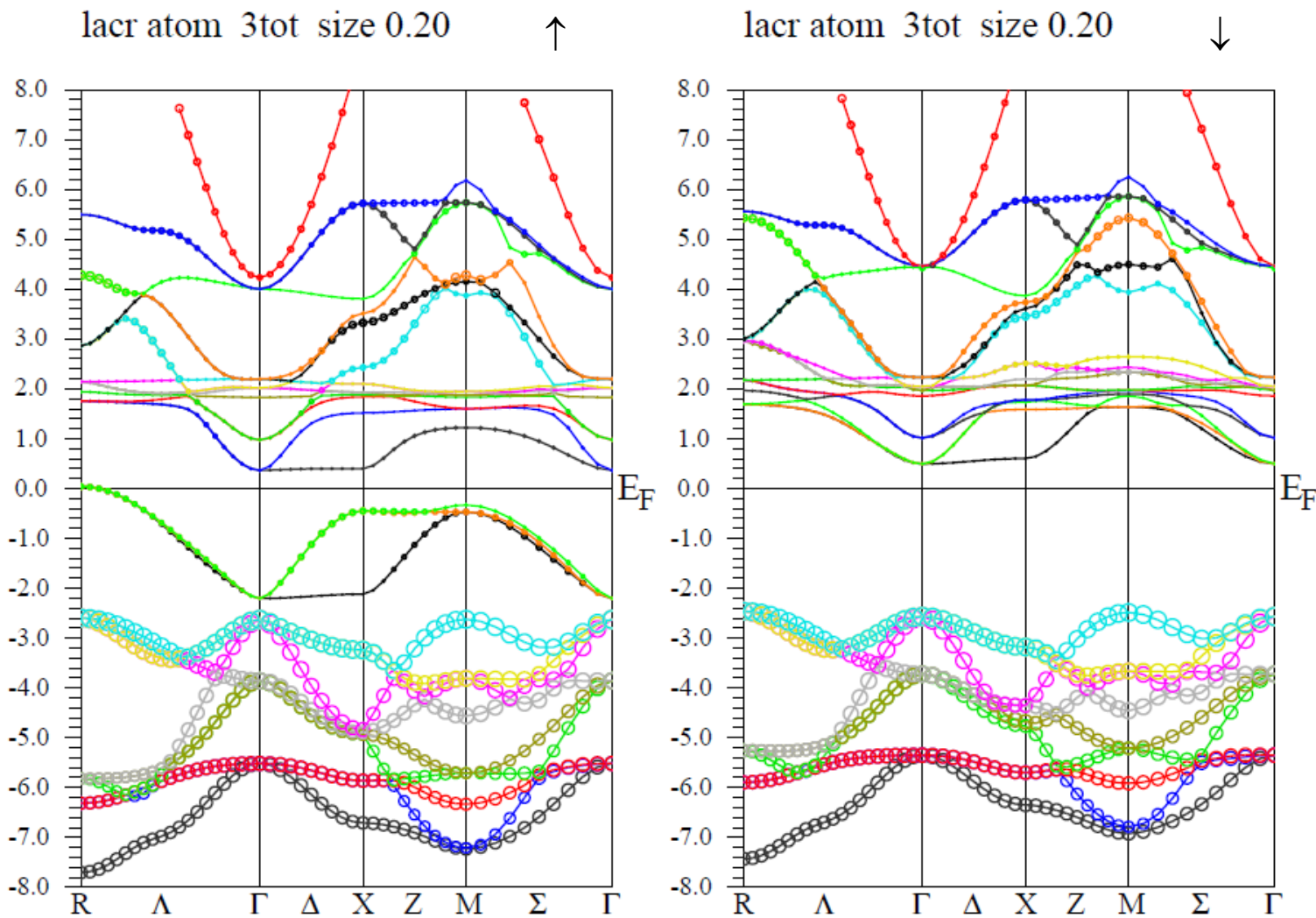
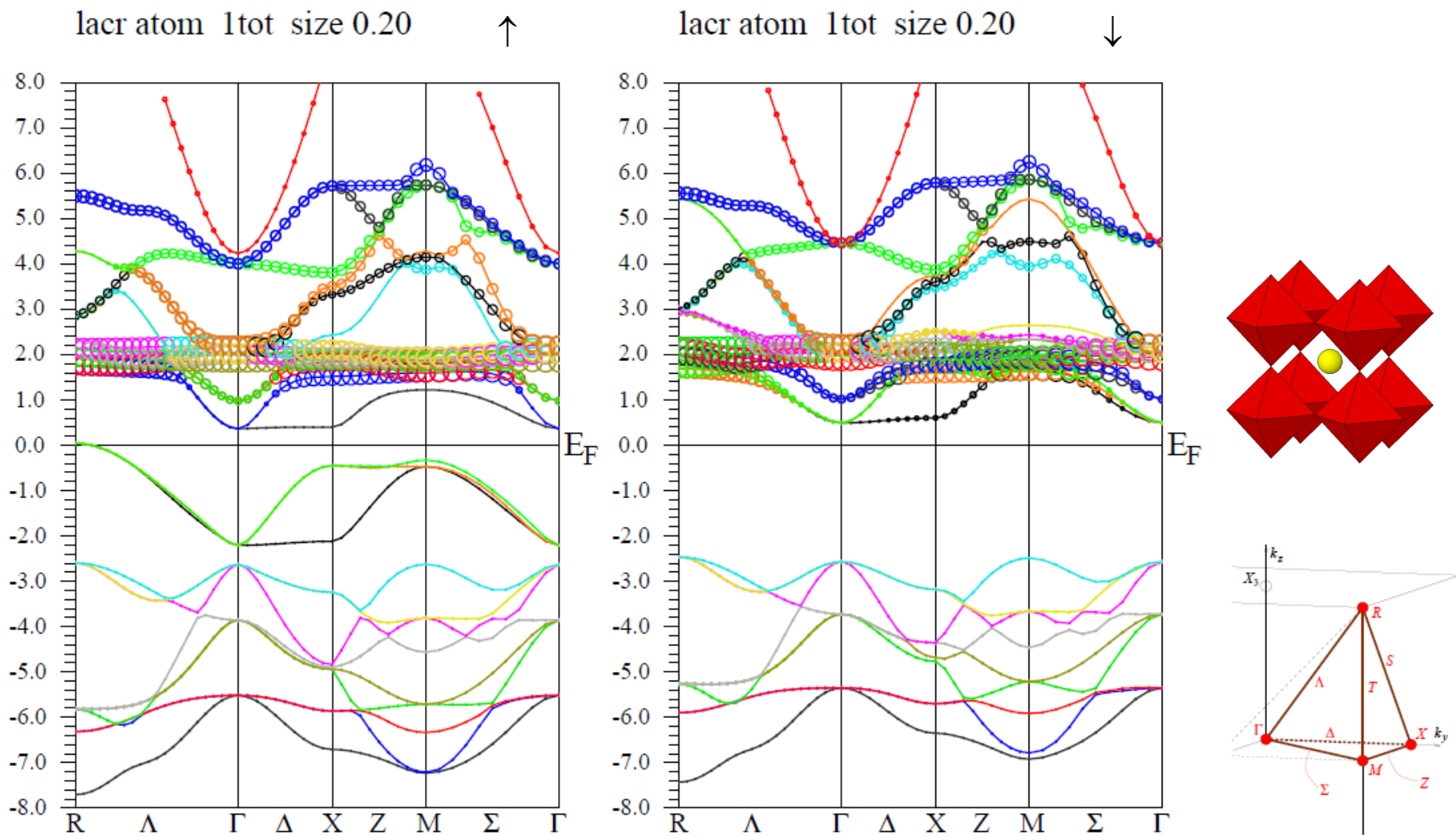
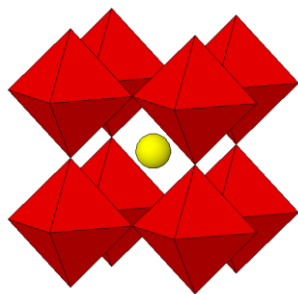
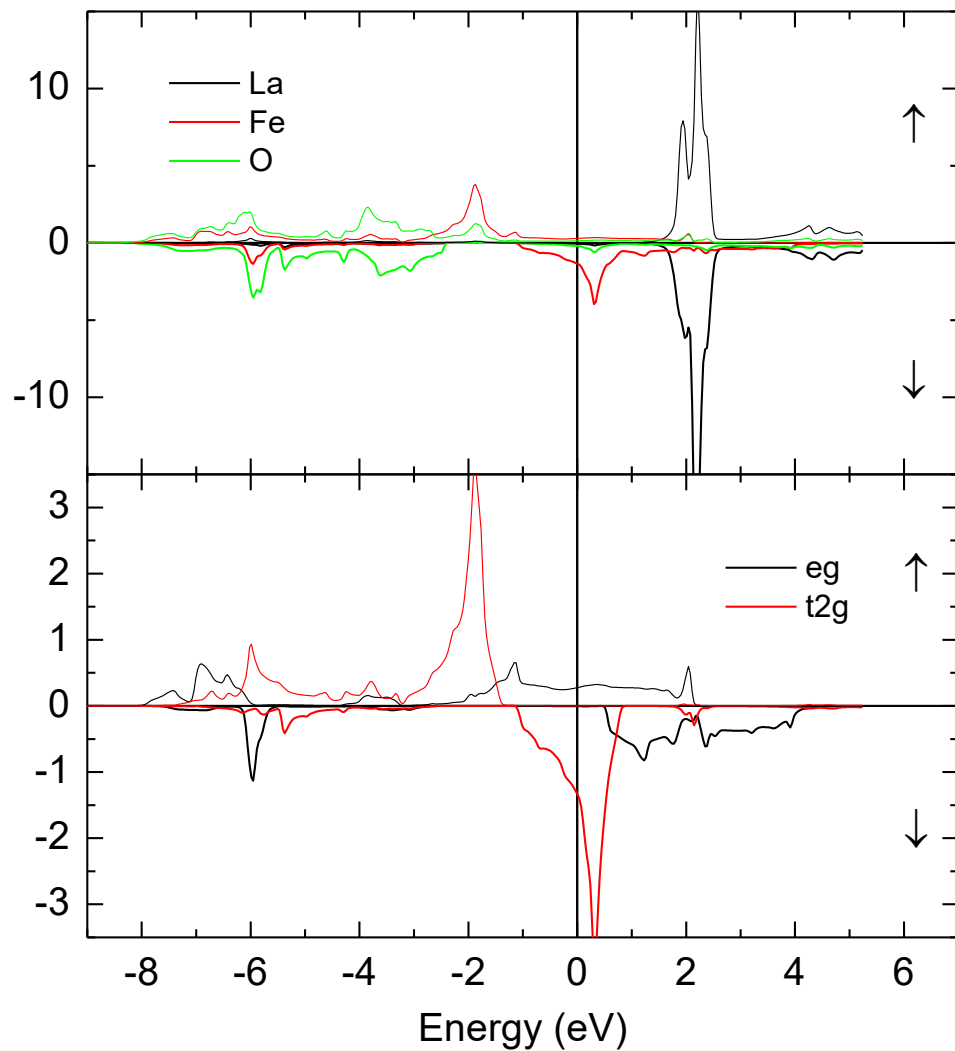


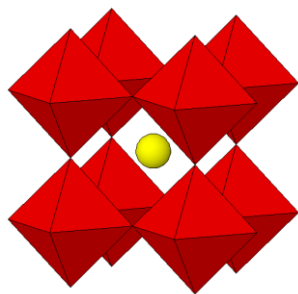
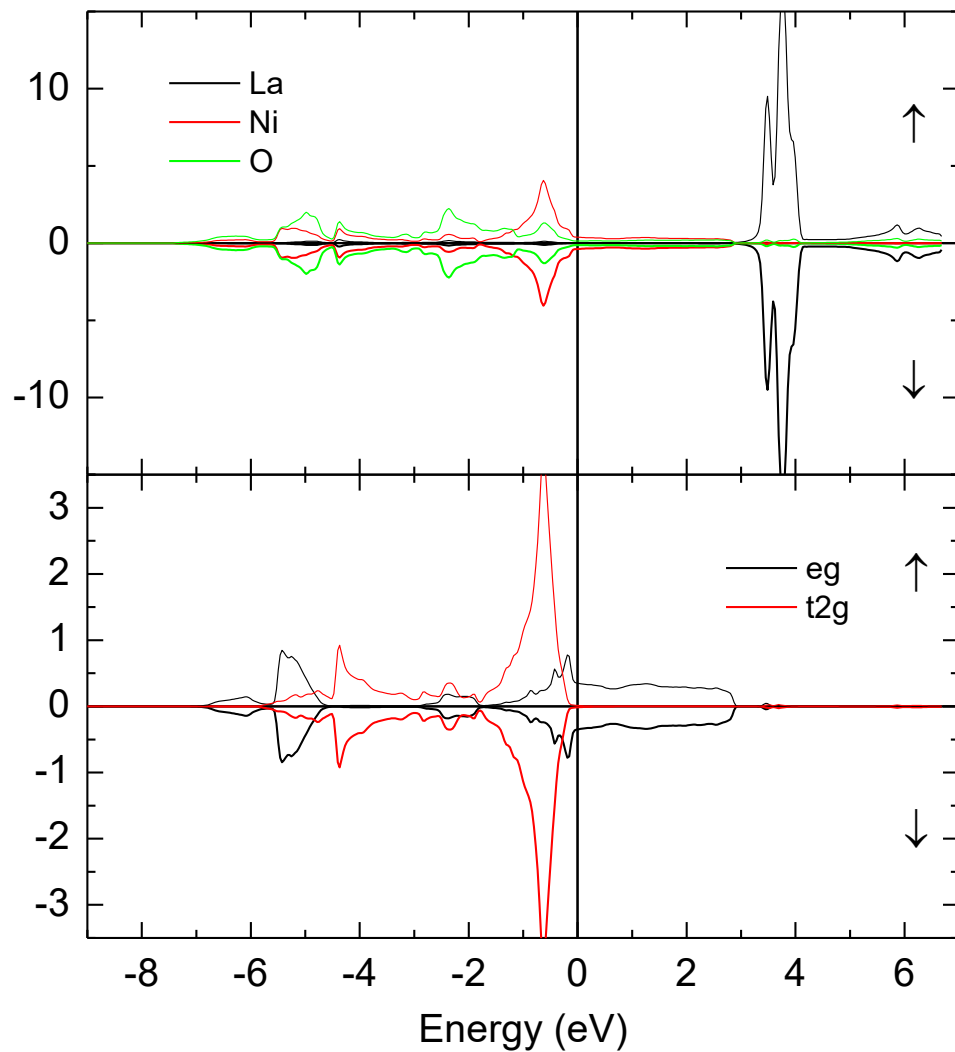
Figure 4: LaCrO₃, d³ – t_{2g}³, O

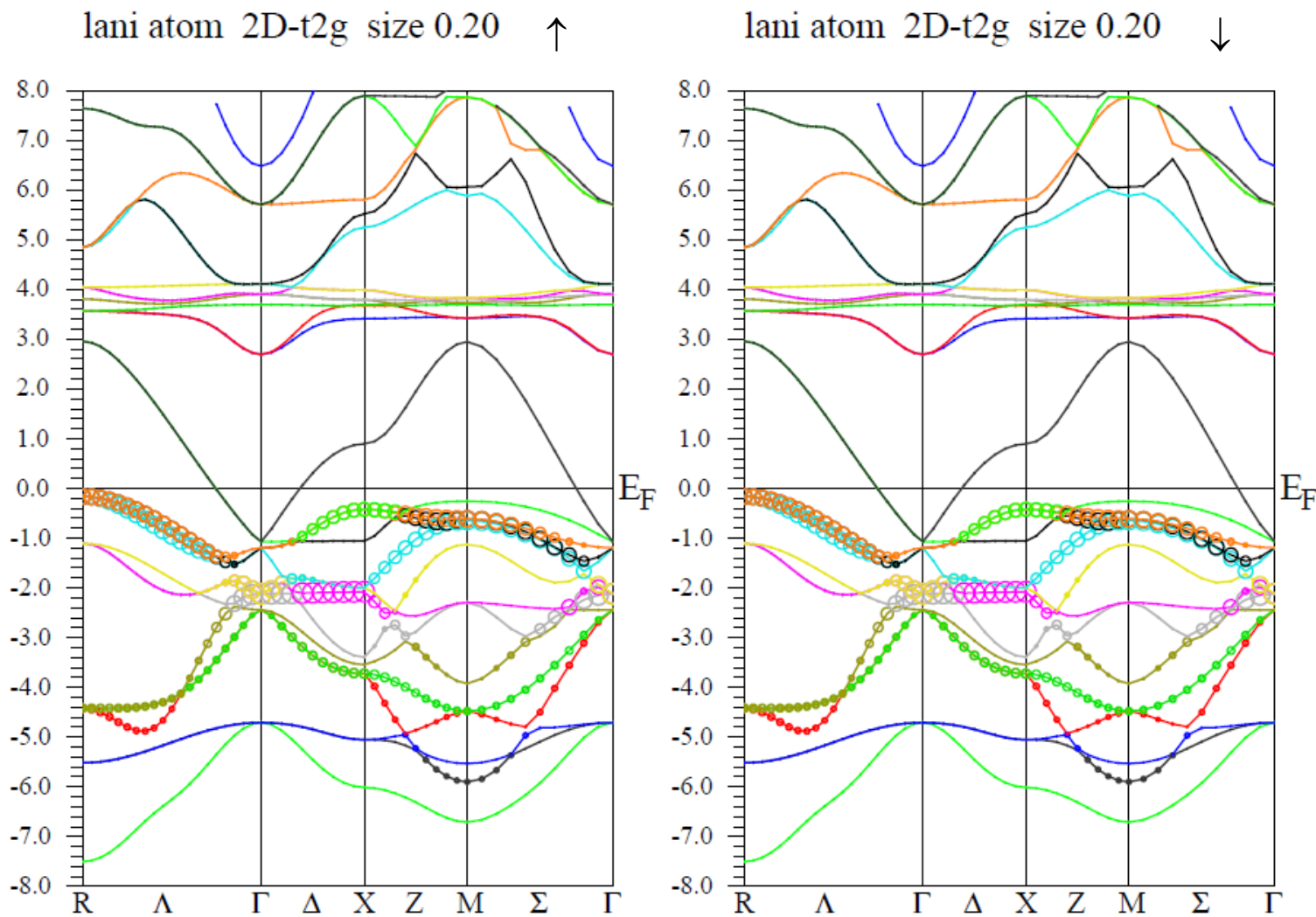
Figure 5: LaCrO₃, $d^3 - t_{2g}^3$, La

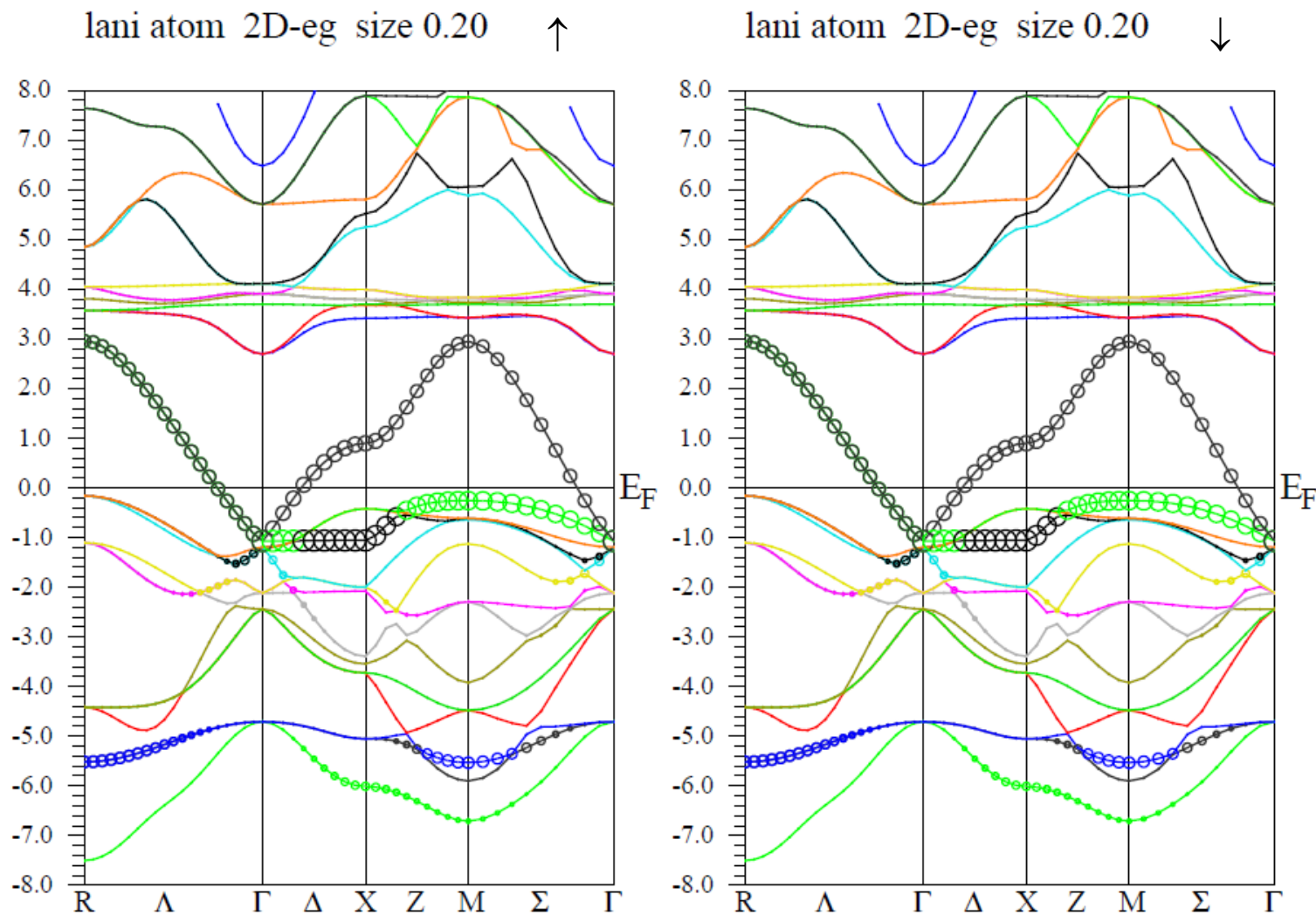
LaFeO₃
d⁵ – t_{2g}³e_g²
vysoký spin



LaNiO₃
d⁷ – t_{2g}⁶e_g¹
nízký spin



Figure 6: LaNiO₃, d⁷ – t_{2g}⁶e_g¹, Ni-t_{2g}

Figure 7: LaNiO₃, $d^7 - t_{2g}^6 e_g^1$, Ni- e_g

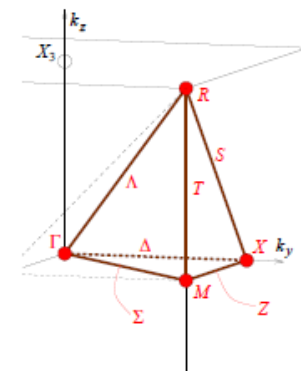
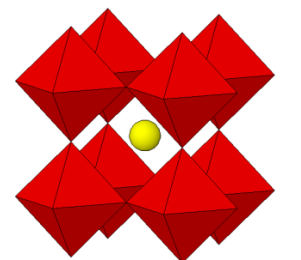
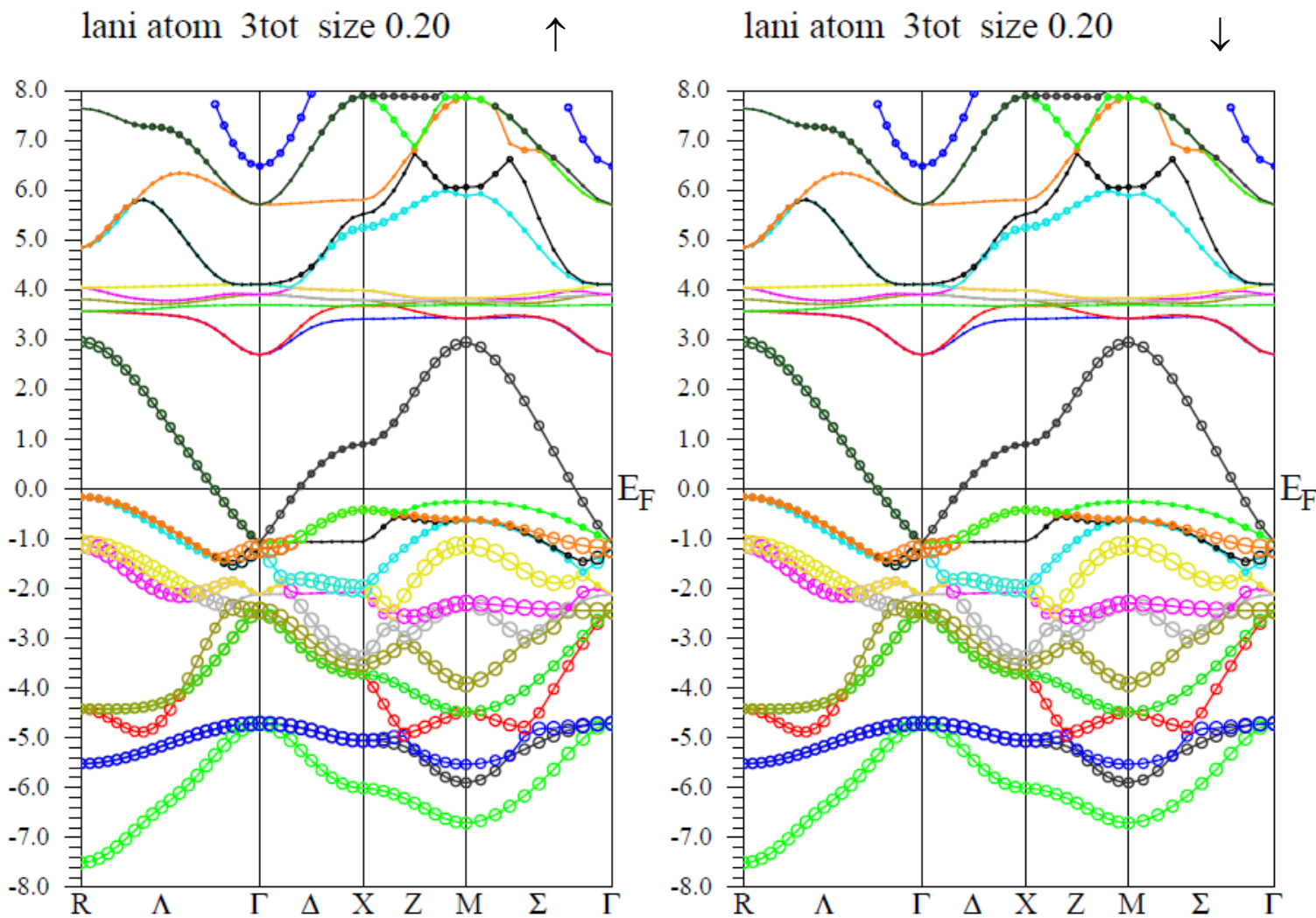
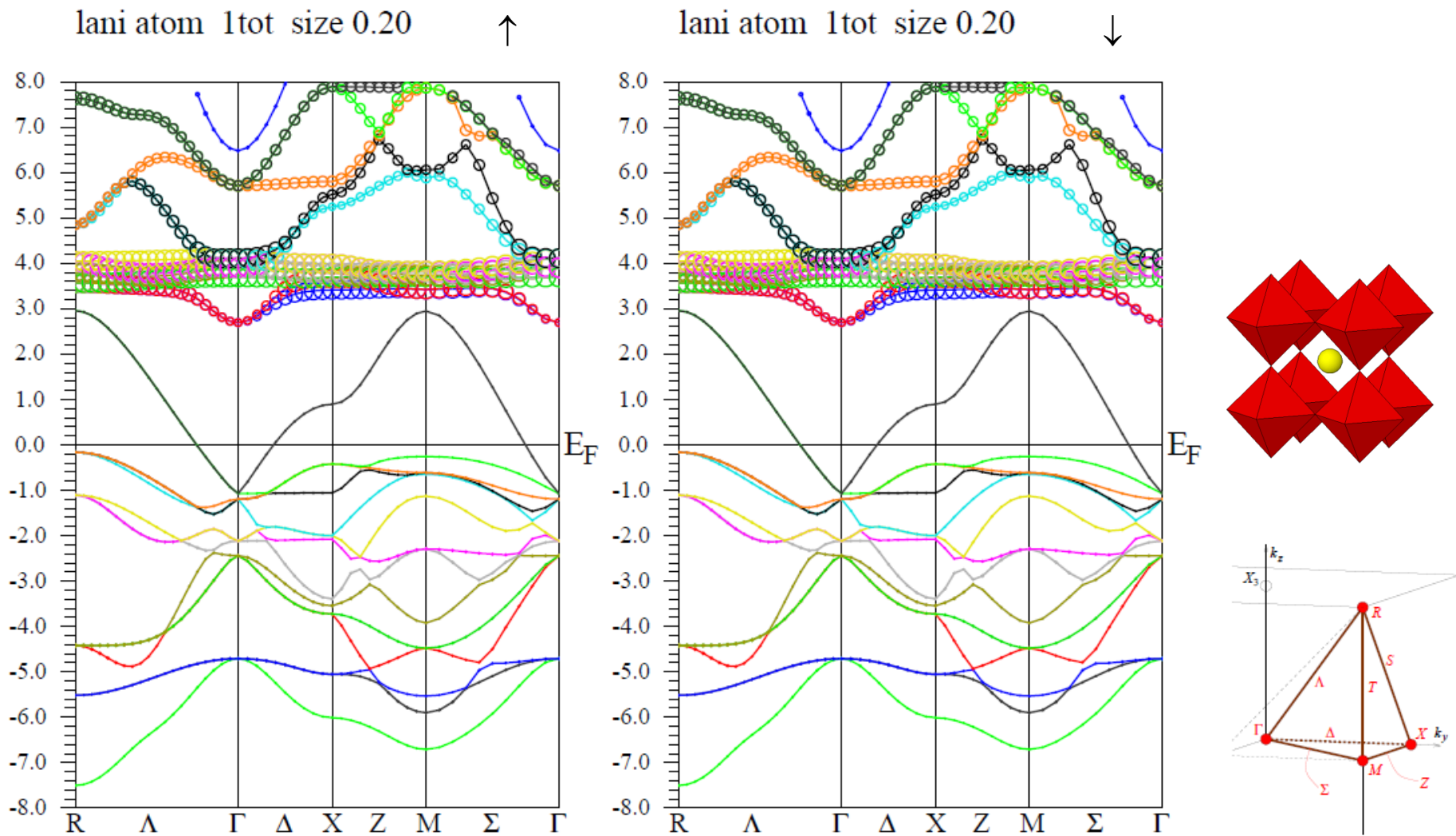


Figure 8: LaNiO₃, $d^7 - t_{2g}^6 e_g^1$, O

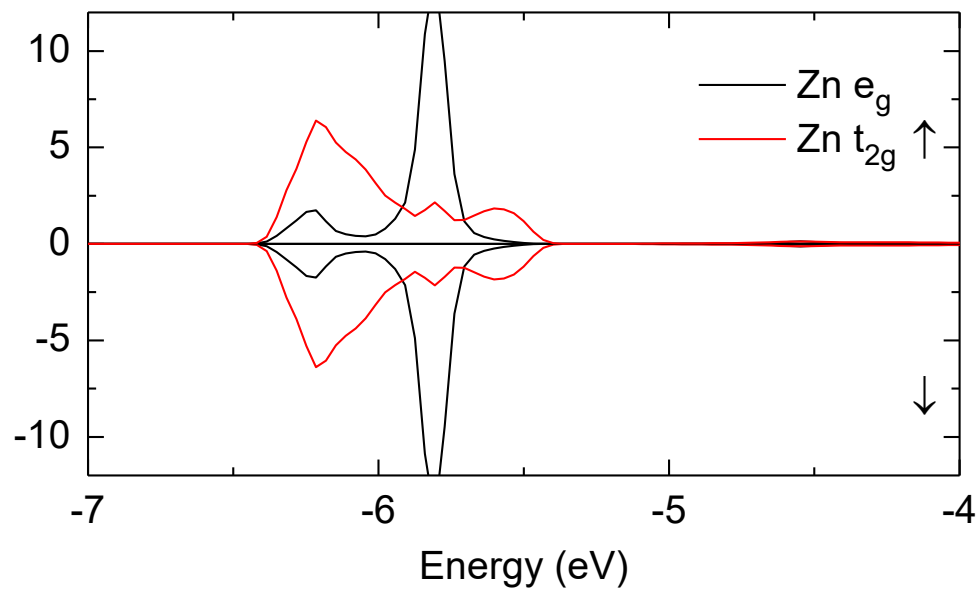
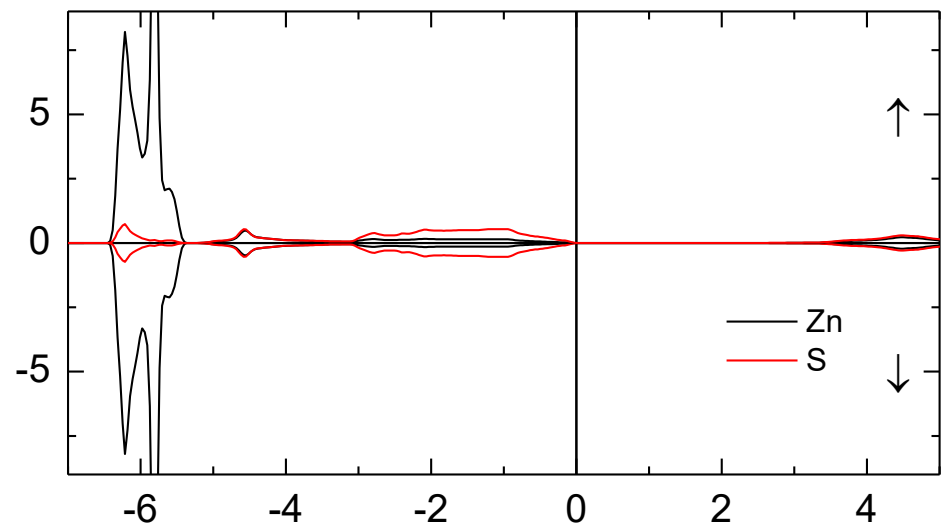
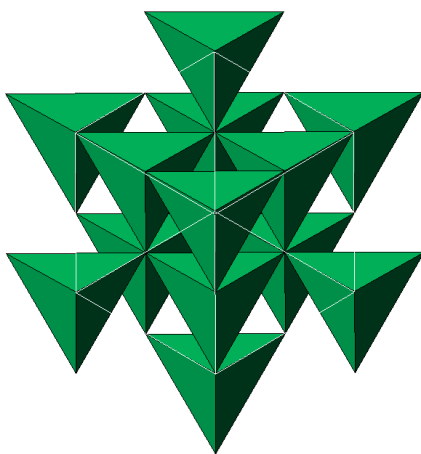
Figure 9: LaNiO₃, $d^7 - t_{2g}^6 e_g^1$, La

ZnS - sfalerit

Zn: $d^{10} - t_2^6 e^4$

F43m

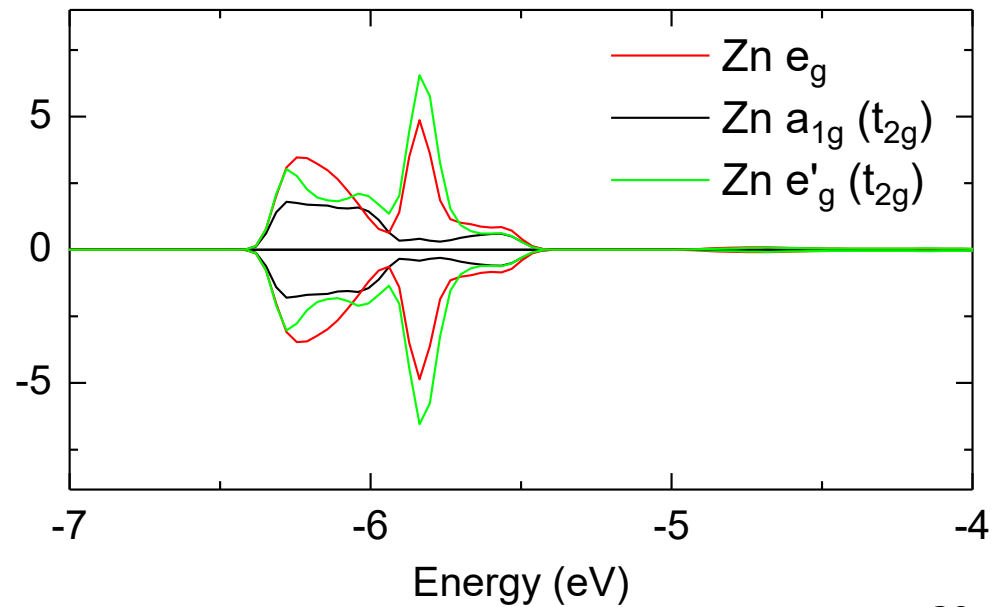
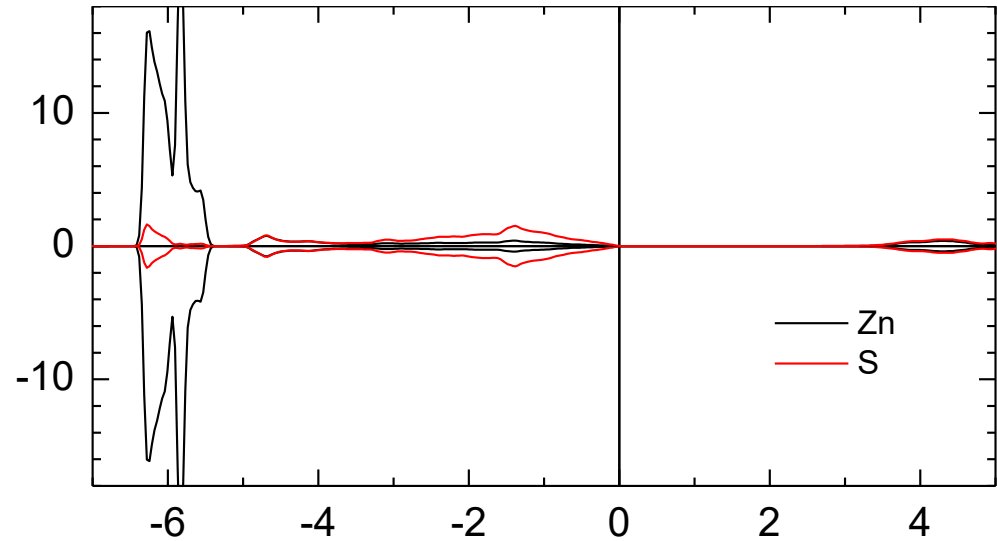
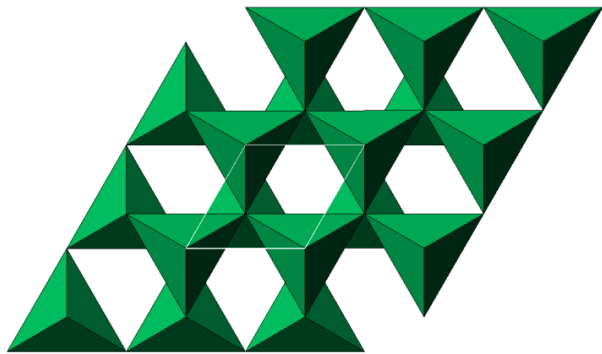
tetraedr



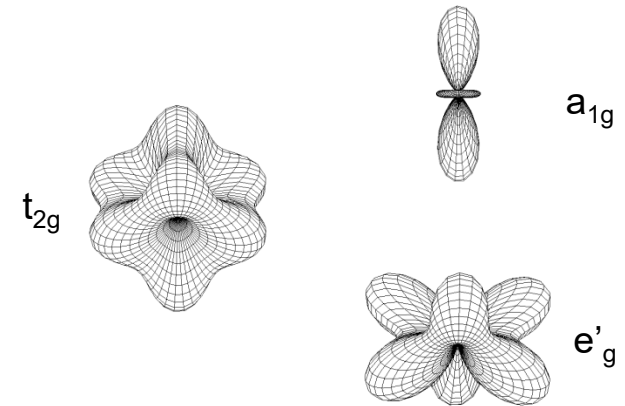
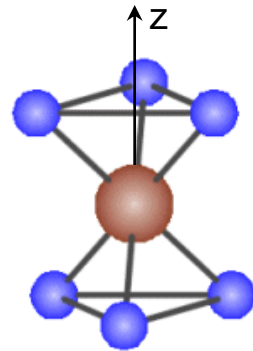
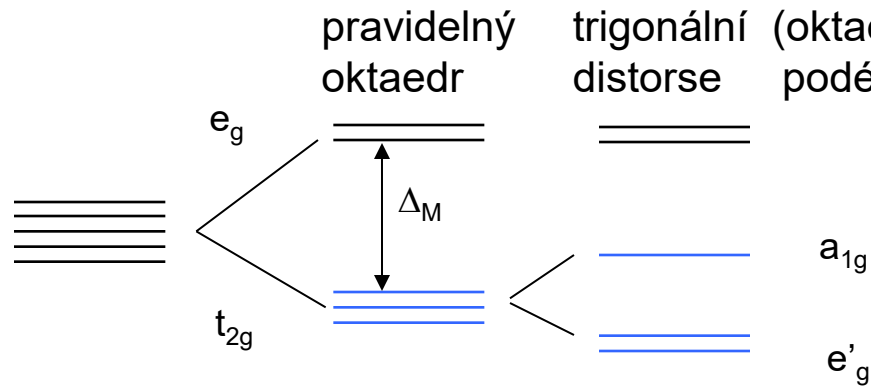
ZnS - wurtzit

Zn: d^{10} – trigonální štěpení $P6_3mc$

tetraedr

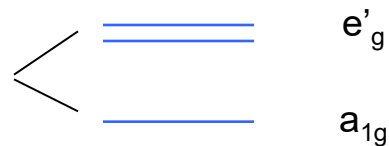


V trigonálně distortovaném oktaedru se t_{2g} orbital dále štěpí na a_{1g} a e'_g .

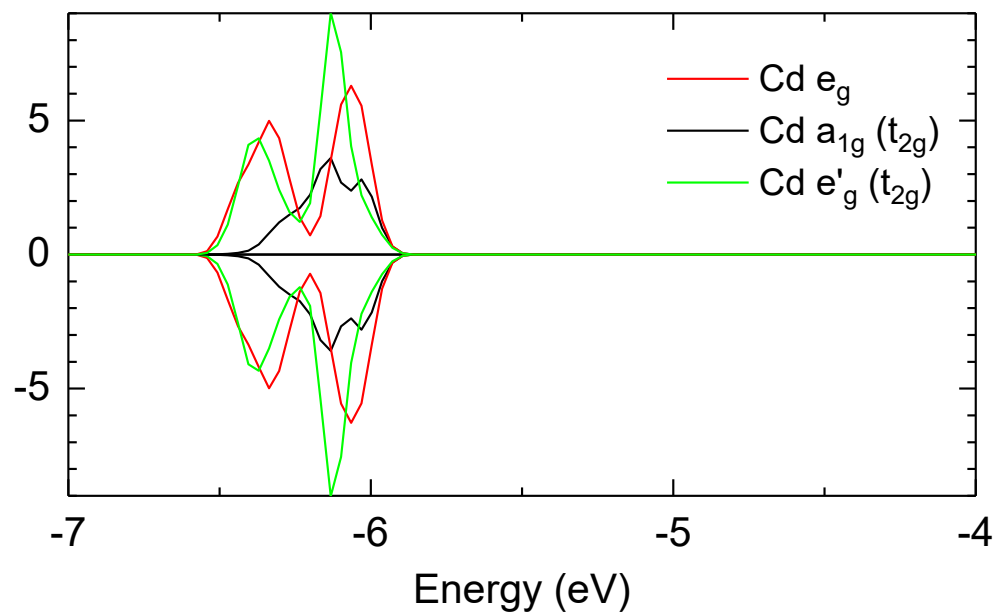
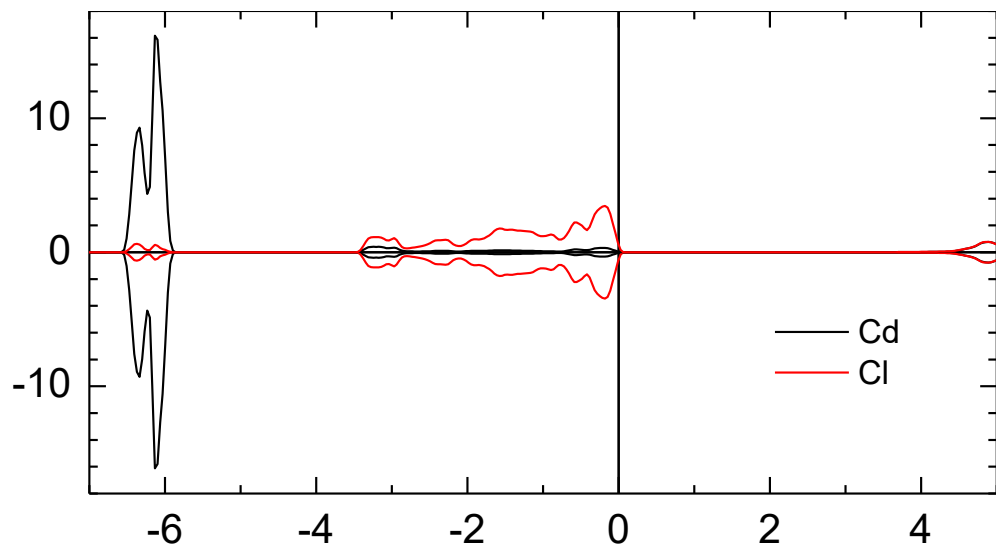
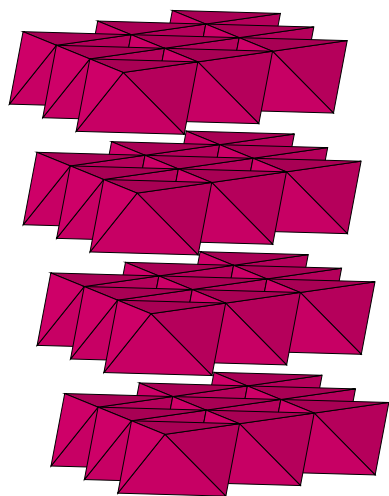


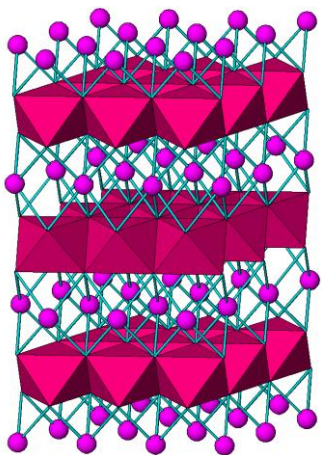
stlačený oktaedr: např. $CdCl_2$, $NaCoO_2$.
 protažený oktaedr: např. Fe_3O_4 .

(oktaedr protažený podél trigonální osy z)



CdCl₂
 Cd: d¹⁰ – trigonální štěpení
 R3m
 oktaedry spojené hranami





Co d (6)



e_g (0)

$d_{z^2}+d_{x^2-y^2}$ (e_g)

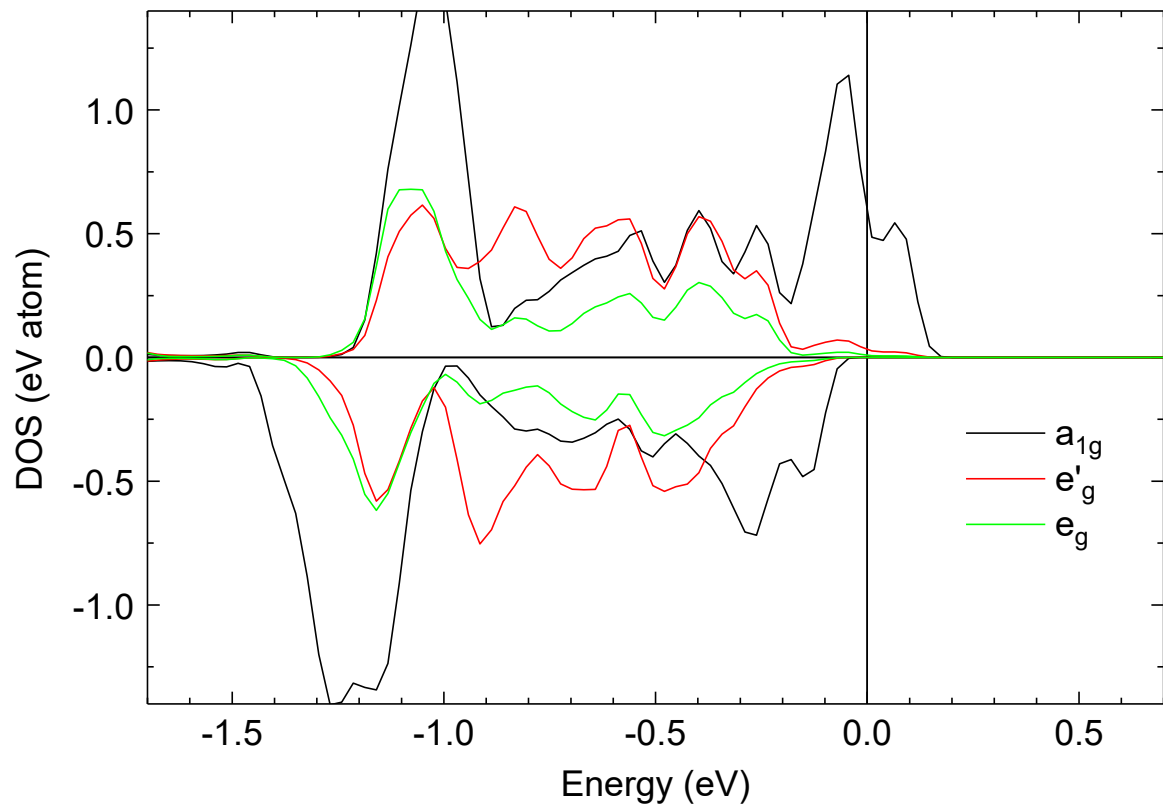


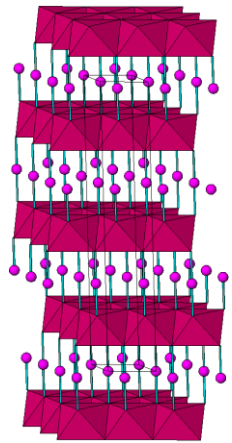
a_{1g} (2)

$d_{xy}+d_{xz}+d_{yz}$ (t_{2g})



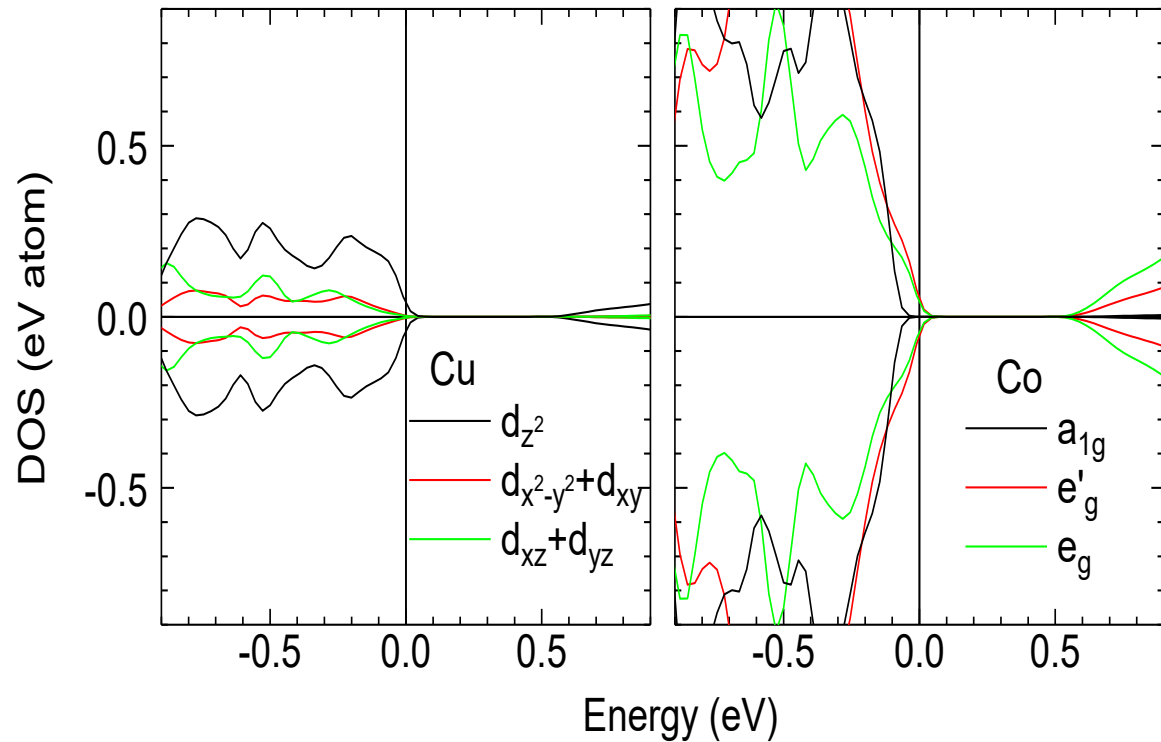
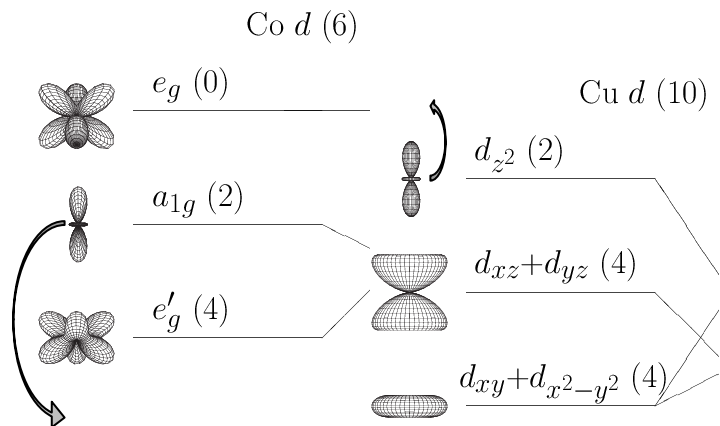
e'_g (4)





CoO₆ trigonálně
deformované
oktaedry
Cu v lineární
koordinaci

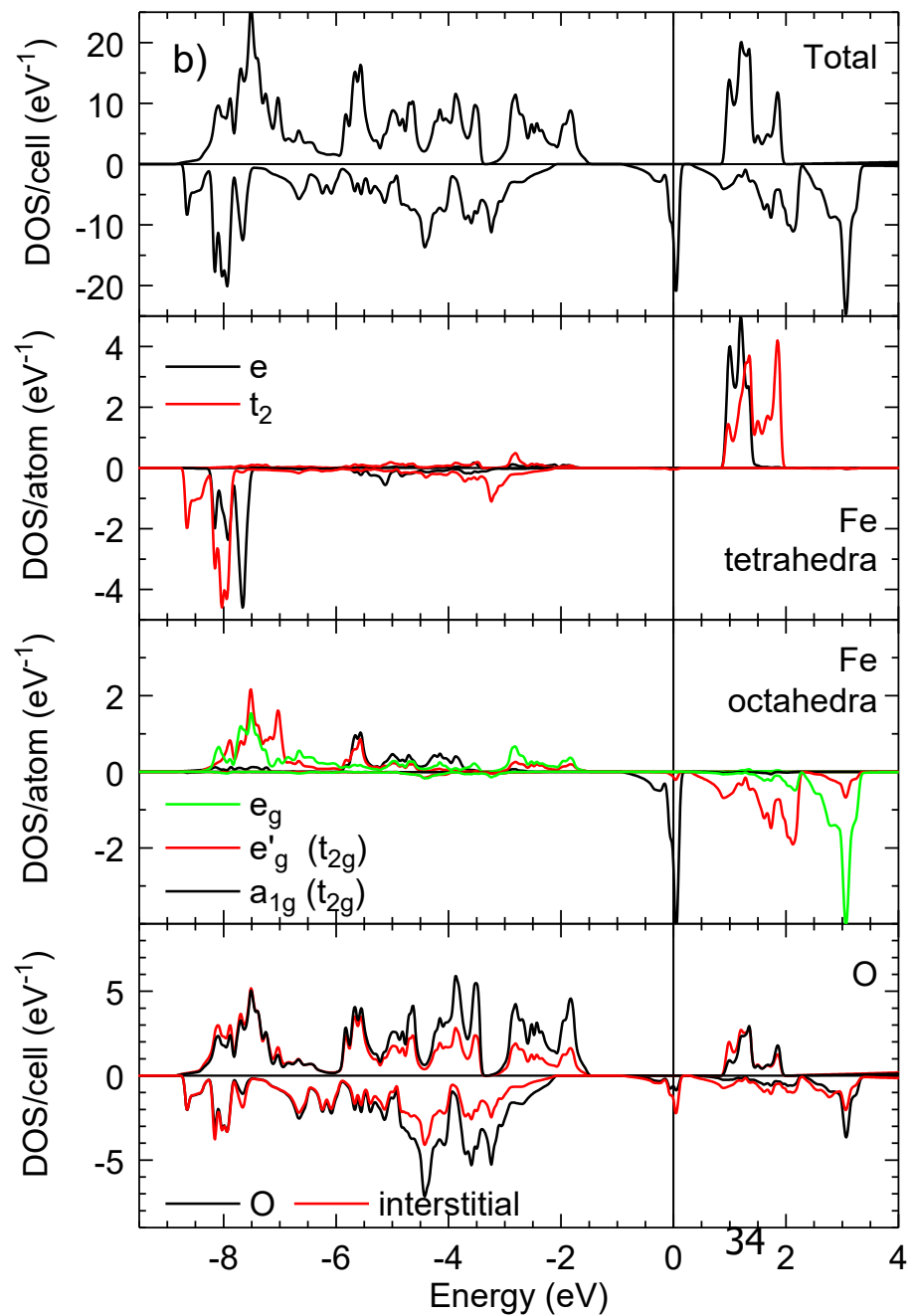
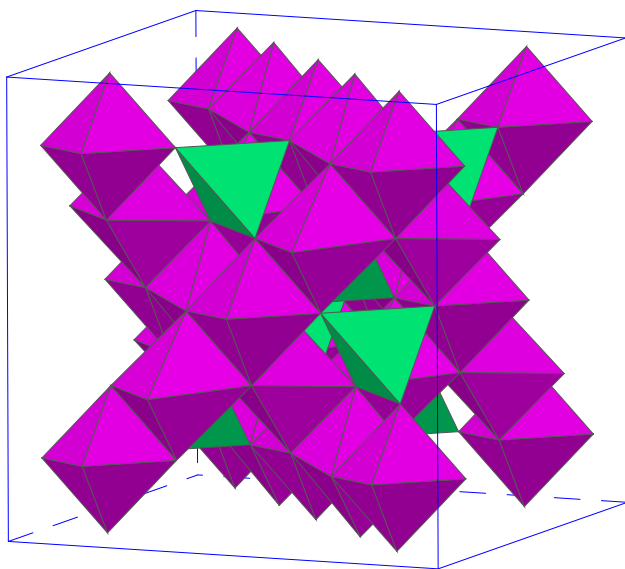
hybridizace Co- a_{1g} a Cu- d_{z^2} .



The band structure of CuCoO₂ is influenced by the hybridization between symmetrically related Co- a_{1g} and Cu- d_{z^2} orbitals, which pushes the Co- a_{1g} orbital down below the Fermi level, so that bands at E_F have the Co- e'_g and e_g character.

This is in contrast to the band structure of thermoelectric material Na_xCoO₂, where the band crossing Fermi level has the a_{1g} character, in accordance with one-electron levels splitting in the crystal field of trigonal coordination compressed along the z -axis.

Fe₃O₄, magnetit
spinelová struktura



Fe₃S₄, greigit
spinelová struktura

